....

COURSE 1

ntMESOSCOPIC LIGHT SCATTERING IN ATOMIC PHYSICS

B.A. VAN TIGGELEN

Laboratoire de Physique et Modélisation des Systèmes Condensés, CNRS/Université Joseph Fourier, B.P. 166, 38042 Grenoble Cedex 09, France

PHOTO: height 7.5cm, width 11cm

Contents

1

B.A. van Tiggelen

Waves always behave in a similar way
(Léon Brillouin, in: Wave Propagation and Group Velocity, 1960)

1 Introduction

The recognition of wave propagation in daily life goes back a long time ago. The first serious mathematical descriptions - put forward in the context of light propagation - were due to Huygens (1690), who formulated the famous Huygens' principle and Fresnel (1810) who derived this principle from a wave equation. With the formulation of Maxwell's equations for electromagnetic waves by the end of the 19th century, the wave concept found its first spectacular application in physics.

This century may again be called the century of the wave. During the last century, quantum-mechanical wave behavior of first electrons and later atoms and even entire macroscopic material objects, such as superconductors, superfluids and Bose-Einstein condensates, has been established. The wave concept has undoubtedly become the most important concept in physics. This statement implies that wave mechanics - the theory of wave propagation in space-time - is the most important formalism in physics. The wave concept is what this lecture has in common with other themes of this summer school. The aim of this lecture is to introduce "mesoscopic" scattering theory in atomic physics, using knowledge gathered from classical waves [1], keeping the citation above in mind. Other lectures with regard to this subject have been given [2, 3] with an approach more from the atomic physics point of view, though recognizing the importance of mesoscopic scattering. Mesoscopic physics has been the subject of a Les Houches summer school in 1994 [4]. It has seen a considerable breakthrough in the last 10 years, especially in the context of quantum transport, with the development of its own language of random matrix theory [5].

Only after I had decided to use Brillouin's openings phrase of his famous book as a slogan for my lectures, I realized the highly nontrivial nature of its message. It led me to pose three pertinent questions, namely

1. What is a wave?

2. What means "behave"?

3. What exactly is meant by "similar"?

Mathematically, any object described by a complex number $\psi(A,\phi) = A\exp(i\phi)$ can be called a "wave", its phase in the complex plane ϕ called the phase of the wave, and the absolute value A related to some density $\rho \sim A^2$ of the wave. Complex numbers have the properties that we believe characterize "waves", namely *superposition* (the sum of two waves is again a wave, but the phases do not add), *interference* (the joint density A^2 of two waves is not equal to the sum of the densities, and can actually vanish, i.e. interfere destructively) and periodicity: $\psi(\phi) = \psi(\phi + 2\pi)$.

The answer to the second question refers to a set of rules that govern the propagation of waves in space-time $(\mathbf{r}, t)$. This brings us to the physical aspects of waves, finding applications in almost all domains of physics. In general, the answer depends on the nature of the waves, such as electromagnetic waves, acoustic or elastic (mechanical) waves, De Broglie (matter) waves, or flexural waves (Table I). In principle, the behavior of a wave is completely described by the solution of its wave equation, the density A^2 in all cases proportional to some "conserved quantity" in time. The "similarity" of wave behavior, conjectured by Brillouin, is not evident by looking at Table 1.

WAVE	WAVE EQUATION
Non-interacting Matter Waves Schrödinger equation	$[-\hbar^2\nabla^2/2m + V(\mathbf{r})]\psi = i\hbar\partial_t\psi$ ψ : complex probability amplitude
Linear Electromagnetic Waves Helmholtz equation	$c_0^{-2}\varepsilon(\mathbf{r})\partial_t^2\mathbf{E} + \nabla\times\nabla\times\mathbf{E} = 0$ $\mathbf{E}$: electric field
Mechanical Waves Elastic wave equation	$\rho\partial_t^2\mathbf{s} = (\lambda+2\mu)\nabla\nabla\cdot\mathbf{s}$ $-\mu\nabla\times\nabla\times\mathbf{s}$ $\mathbf{s}$: displacement vector
Flexural waves Euler-Bernouli equation	$\nabla^4\phi + \kappa(\mathbf{r})\partial_t^2\phi = 0$ ϕ : transverse displacement

Table 1 Waves and their behavior.

Despite early successes in the understanding of wave behavior, most of our present knowledge on wave mechanics - scattering theory in particular - was developed during the development of quantum mechanics in the beginning of the 20th century. One crucial property of a wave, the wave number $\mathbf{k}$, describing the phase evolution in space, was related to the momentum $\mathbf{p} = m\mathbf{v}$ of a particle, according to the famous De Broglie relation $\mathbf{p} = \hbar\mathbf{k}$. The phase evolution in time was, via the Schrödinger equation, related to nothing less than the Hamiltonian of the particle. The success of quantum

mechanics has been so impressive that some people think that wave mechanics and quantum mechanics are actually synonymous (note the word "quantum" in Ref. [4]). Many results in quantum mechanics are mere consequences of wave mechanics, and are not "quantum" at all. Real quantum results are related to the specific interpretation of the Schrödinger wave function as a probability distribution and its consequences for the measurement problem, as well as most results of second quantification, where "wave-particle duality" emerges.

The universality of wave mechanics is often obscured by details required to solve a specific problem. In atomic physics one wishes to understand how light interacts with atoms. From the point of view of wave mechanics this problem can be cast into a well-defined scattering problem, creating a "light-in-light-out" set-up. One has in that case integrated out the material degrees of freedom that have been hidden in a S-matrix of the light, a situation that is actually close to the way atomic physics is done experimentally. However, the usual approach in theoretical atomic physics is different, and prefers to integrate out the light waves, leaving us with "dressed" material degrees of freedom, involving electrical polarization, spontaneous emission and Lamb shifts. Even the incident light is transformed into a material property called the Rabi frequency! In general, both pictures are complementary, but to do mesoscopic physics the scattering theory is highly favorite. Many ideas in this course have already been written down in a 1996 review paper [6]. This contribution intends to introduce scattering theory in atomic systems.

2 Mesoscopic wave physics

Wave mechanics is the formalism to describe wave propagation in space and time. Before discussing mathematical details of this theory, it is important to oversee its limitations and universality, and to identify the differences. We can then decide under what conditions waves behave "similarly".

2.1 Mesoscopic quantum mechanics

Central in quantum mechanics is a complex wave field $\psi(\mathbf{r},t)$. The time-evolution is governed by the "energy operator" or Hamiltonian H. The Schrödinger equation of motion and its formal solution are given by,

$$i\hbar\partial_t\psi = H\psi \Rightarrow \psi(t) = \exp(-iHt/\hbar)\,\psi(0)\,. \tag{2.1}$$

From the formal solution it is clear that the phase evolution of the wave in time is directly related to the Hamiltonian. The phase is a crucial property for waves because it is at the base of interference phenomena. Two reasons exist why the "exact" solution really only is a formal solution in practice:

decoherence and randomness. A clear distinction of both aspects is crucial for a comparison of classical waves and "quantum" waves.

The first point is that, for Eq. (2.1) to apply, H must be the *total* Hamiltonian of the system. The hermitean nature of H guarantees that, at all times

$$\langle\psi(t)|\psi(t)\rangle = \int \mathrm{d}\mathbf{r}\,|\psi(\mathbf{r},t)|^2 = 1\,, \tag{2.2}$$

or equivalently, that the density matrix has total trace of unity. In practice, H always contains an unknown coupling to some large system, the "environment", with many degrees of freedom which are, due to lack of knowledge, described by a statistical mixture. In the world whose H we know and whose properties we want to study, energy is not conserved, and processes are inelastic. Because Eq. (2.1) relates the energy directly to the phase evolution in time, a characteristic *inelastic time* τ_ϕ exists, beyond which all interference phenomena will be destroyed by dephasing inelastic effects. A possible definition of the inelastic time is,

$$\frac{\langle\psi(\mathbf{r},t)\psi^*(\mathbf{r},t+\tau)\rangle}{\langle\psi(\mathbf{r},t)\psi^*(\mathbf{r},t)\rangle} \sim \exp(-\tau/\tau_\phi)\ . \tag{2.3}$$

In atomic physics the left hand side of this definition is known as the *first order coherence function* $g_1(\tau)$ [16]. The averaging carried out in definition (2.3) addresses the unknown degrees of freedom, such as vacuum fluctuations, randomly passing phonons, or atomic collisions, that have been integrated out ("traced over"). Beyond the time τ_ϕ there is no point doing quantum mechanics anymore: the phase is scrambled and only phase-insensitive, classical effects remain. The "reduced" density matrix, obtained after having integrated out the unknowns, *remains normalized to unity*, when traced over the known degrees of freedom. The destruction of phase (more technically speaking off-diagonal elements in the density matrix) by the coupling with a large environment is called *decoherence* [7]. It is discussed in detail by W. Zurek and J. Paz in this book.

To give an order of magnitude, $\tau_\phi \approx 10^{-11}$ s for a copper wire at T=1 K. With a Fermi velocity of 10^6 m/s this corresponds to a dephasing length of $\ell_\phi = 10\,\mu$m. This length explains immediately why phase plays no role for normal ohmic conduction. On the other hand, this dephasing length is still large enough compared to the lattice spacing for the electrons to benefit from constructive Bloch interferences. Since $\tau_\phi \sim 1/\delta E$, with δE typical fluctuations of system energy, we estimate that $\tau_\phi \sim 1/kT$ at temperature T, which is typically what is found for electron-phonon coupling [8]. Hence, cooling down is the way to enter the regime where the phase comes in.

The role of disorder is less dramatic, but nevertheless as important. The known part of the Hamiltonian is often only known in a statistical way. For instance, it describes s-wave impurities in a semi-conductor, whose exact

locations we do not know. Yet, they are *not* integrated out, but treated in a probabilistic way. No inelastic scattering exists and the phase is not destroyed, just randomized in a way that we should be able to figure out. This means that interference phenomena can still persist on all length scales, although the wave number is no longer a conserved quantity as it was in a homogeneous medium. The dephasing caused by randomization of the wavenumber is described by another length scale, called the *extinction mean free path* ℓ. In terms of a solution at energy E it can be defined as,

$$\langle \psi(\mathbf{r},E)\psi(\mathbf{r}+\mathbf{x},E)^*\rangle \sim \exp(-x/2\ell(E))\,. \tag{2.4}$$

The averaging is now performed over random variables in the known Hamiltonian. The *extinction mean free time* τ is readily defined as $\tau = \ell/v$ with v the wave velocity. The factor of 2 in Eq. (2.4) is included to guarantee that for a source at $\mathbf{r}$ the density $|\,\langle\psi(\mathbf{r}+\mathbf{x})\rangle\,|^2$ decays as $\exp(-x/\ell)$, a law that is in optics referred to as Beer's law. In a copper wire at 1 K, the mean free path caused by electron-impurity scattering amounts to $\ell \approx 5$ nm, much smaller than the inelastic length, but only one order of magnitude bigger than the De Broglie wavelength λ_B.

The confusion between dephasing processes caused by decoherence and randomness is due to bad but unfortunately irreversible terminology. For instance, classical light scattered from a random medium like Teflon or fog is regularly called "incoherent" by optical physicists, because the phase is randomized. However, this "incoherent" signal is as coherent as the incident light, according to the proper definition in atomic physics, using the coherence function $g_1(\tau)$. The phase is just a random variable. By studying for instance "speckles" (intensity fluctuations) a lot of information on randomess can be retrieved. This is much more difficult - if not impossible - for decoherence processes.

If Δt is the typical time the wave spends in the medium, the regime,

$$\frac{\hbar}{E} < \tau < \Delta t < \tau_\phi \qquad \text{(De Broglie waves)} \tag{2.5}$$

is called the *mesoscopic regime* for matter waves, a regime located in between "macroscopic" ($\Delta t > \tau_\phi$) and "microscopic" ($\Delta t < \tau$), but with best of both worlds [4]. The time scales Δt, τ_ϕ and τ can be called "*the good, the bad and the ugly*", after a famous Eastwood western: Δt is "good" because it is under control experimentally; τ_ϕ is bad for it destroys something beautiful; Finally, τ is ugly because multiple scattering and disorder are often a nuisance, but they are just a nuisance. The last inequality sign guarantees the pertinence of phase throughout the sample. The second inequality implies that the system is sufficiently disordered to have multiple scattering. The first inequality is a rough criterion for Anderson localization (in three dimensions) to set in, and locates a completely different regime in wave

propagation, which I - contrary to others [4] - wish to exclude from the mesoscopic regime. In this regime, the phase has induced a genuine phase transition, called Anderson localization. Localization of waves has been discussed in a former Les Houches lecture [9], where all important references can be found.

2.2 Phenomenological Radiative Transfer

For almost one entire century, the standard way to describe multiple scattering of light has been by means of the *equation of radiative transfer*. This equation ignores any possible interference, treating waves as classical particles, and reads [10]

$$\frac{1}{c}\partial_t I_{\mathbf{k}}(\mathbf{r},t) + \hat{\mathbf{k}}\cdot\nabla I_{\mathbf{k}}(\mathbf{r},t) + \left(\frac{1}{\ell}+\frac{1}{\ell_a}\right) I_{\mathbf{k}}(\mathbf{r},t) = \frac{\varepsilon(\mathbf{r},t)}{4\pi} + n\int \mathrm{d}\hat{\mathbf{k}}'\,\frac{\mathrm{d}\sigma}{\mathrm{d}\Omega}(\mathbf{k}'\to\mathbf{k}) I_{\mathbf{k}'}(\mathbf{r},t)\,, \tag{2.6}$$

featuring the local *specific intensity* $I_{\mathbf{k}}(\mathbf{r},t)$, i.e. the local energy flux density propagating in direction $\mathbf{k}$. Equation (2.6) is a book-keeping and treats a number of processes in a phenomenological way. The first two terms describe a volume element "co-moving with the light". The third "loss" term contains two parts. The *coherent* loss term $1/\ell$ describes light that is scattered elastically out of the forward beam, featuring the scattering mean free ℓ; the *incoherent term* $1/\ell_a$ is a genuine sink term and describes loss of light. Similarly, the righthand side contains two "gain" terms. The term ε represents a source term that creates light (i.e. by inelastic atomic transitions). Finally, the last term describes the amount of light (per unit volume) that is scattered elastically into the direction $\mathbf{k}$, with n the number density of scatterers. Two extreme cases can be considered.

If scattering can be neglected, the equation of radiative transfer contains a sink term $1/\ell_a$ and a source term ε. If both are constant in space, and if energy flow is stationary, this simplified case can be solved easily by introducing the so-called source function $S = \varepsilon\ell_a/4\pi$. In (local) thermal equilibrium, absorption and emission can be related, with the result that S is essentially equal to the Planck function $B_\lambda(T)$. This is the celebrated *Kirchoff theorem*. The solution to Eq. (2.6) is in good approximation,

$$I_{\mathbf{k}}(\mathbf{r}) \approx B_\lambda[T(\mathbf{r}-\hat{\mathbf{k}}\ell_a)]\,, \tag{2.7}$$

i.e. it equals the Planck function corresponding to the local temperature of the spot one mean free path away along the line of light. This simple notion explains why stars radiate more or less as black bodies. It also explains why most atomic transitions in the Solar atmosphere are observed *in absorption*: these transitions have a relatively small mean free path so that emerging

photons originate from relatively cool layers of the Sun, for which $B_\lambda(T)$ is relatively small.

On the other hand, if absorption and emission are negligible, all light is scattered elastically. The resulting equation is still very complex, and its solutions have been studied numerically in great detail [11]. It is this situation for which the neglect of phase is not necessarily legitimate. In the next section I will address this question in more detail.

2.3 Mesoscopic physics with classical waves

The classical, macroscopic Maxwell equations contain constitutive constants such as the dielectric constant and the electric conductivity, and should describe the electromagnetic field on scales much bigger than atomic scales. These "constants" do not contain *all* information. Especially in the solid state, where the density of the atoms is high, radiative oscillators couple to a large number of non-radiative decay channels, giving rise to loss of energy. These losses are bigger than $\hbar\omega$ so that photons really disappear in great numbers, in an entirely classical way. In classical wave equations, "energy" is not directly related to time evolution of phase, as we have seen for De Broglie waves. Hence, no reason exists that the phase of a classical wave be scrambled. I emphasize the importance of "classical" to this statement. As soon as classical waves are "quantized", the energy takes over again the role of time evolution. Classically, a phase relation persists between incident and elastically scattered light (i.e the scattered light is "phase locked" to the incident wave), and phase can be measured as long as the amplitude is still large enough for detection. If the time τ_a is the typical absorption time, the mesoscopic regime for classical waves can now be defined as,

$$\frac{2\pi}{\omega} < \tau < \Delta t < \tau_a \qquad \text{(classical waves)}\,. \tag{2.8}$$

The last inequality guarantees the wave to survive. For classical waves the relation

$$\int \mathrm{d}\mathbf{r}\, W(\mathbf{r},t) = \exp(-t/\tau_a)\,, \tag{2.9}$$

holds, where the energy density $W(\mathbf{r},t) \sim |\psi(\mathbf{r},t)|^2$ is proportional to the classical field amplitude squared. This relation is to be contrasted against relation (2.2) for De Broglie waves. Equation (2.9) expresses the fact that *non-radiative decay channels have not been included at all* into the equation. They have not even been integrated out as was done in Eq. (2.2) with the unknown degrees of freedom for matter waves, for that would have led to conservation of W in time. Classically, the simple discard of non-radiative degrees of freedom is possible, since W is not interpreted as "probability density".

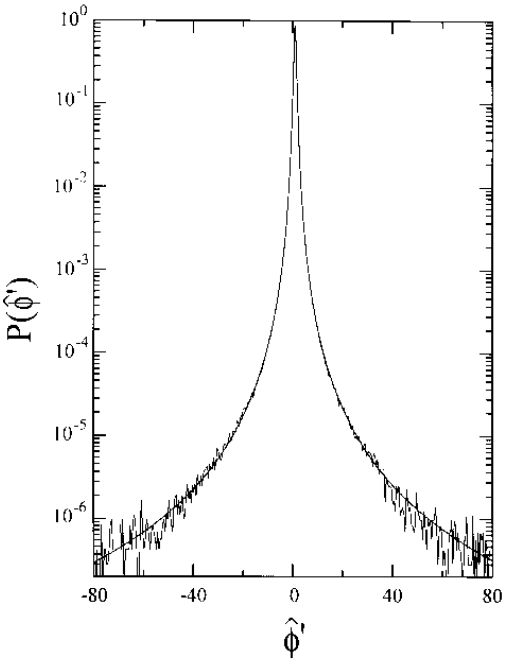

Fig. 1. A recent experiment with classical waves, demonstrating the pertinence of phase in the mesoscopic regime, despite multiple scattering. Microwaves experiments have direct access to the wave. The figure shows the probability distribution of the frequency derivative of the phase shift of microwaves (wavelength 1.5 cm) in transmission from a tube of 1 meter in length, containing 0.5-inch polystyrene spheres (mean free path of 5 cm). Note the high accuracy of more than 1 ppm. The frequency derivative of phase shift is intimately related to "delay time" of the waves in the medium, as explained in section 3. Taken from Genack, Sebbah, Stoychev and Van Tiggelen (1999) [13], with thanks to Azriel Genack.

In general, matter waves and classical waves seem to be much less "similar" than Brillouin wanted us to make believe. Research in the last decades established that only in the regimes described by the criteria (2.5) and (2.8), classical waves and matter waves behave in a surprisingly universal, so-called "mesoscopic" way. The similarity of wave propagation in the mesoscopic regime makes studies with classical waves and matter waves *complementary*, for "similar" does not mean "identical". Dispersion laws are still different, and also charge and spin constitute notable differences, with large impact even in the mesoscopic regime.

The mesoscopic regime is much easier to enter with classical waves. For light propagation in semiconductors (and with frequencies inside the electronic gap to avoid electronic transitions) the absorption length can be as large as centimeters, whereas at the same time the mean free path can be submicron, just at room temperature. This leaves us with four (!) orders of magnitude for the path length $c \times \Delta t$ to do mesoscopic physics. The present world record for the mean free path is $\ell = 0.17\,\mu$m for infrared light in GaAs powders [12]. This small value actually violates the first inequality of criterion (2.8), which offers the possibility of Anderson localization in this system.

In Figure 1 I show the outcome of a recent mesoscopic experiment, demonstrating the pertinent role of phase in the multiple scattering regime [13]. Another typical experiment (see Figure 9), where the phase itself is monitored in the multiple scattering regime - involving coherent backscattering - will be discussed in section 4. These mesoscopic experiments confirm that the phase is not destroyed by multiple scattering, but just randomized. Microwaves and acoustic waves facilitate a direct measurement of the phase. The high frequencies of light enable only indirect phase studies, focusing on flux or energy density.

2.4 Mesoscopic light scattering in atomic gases

The first study of multiple light scattering in resonant atomic systems is due to Compton in 1922 [14] and was refined in 1947 by Holstein [15] in a really outstanding paper. The question raised by Compton and Holstein was how light will propagate in a gas with atoms more or less resonant with the light. If the medium is bigger than the mean free path, emitted photons will be rapidly recaptured by other atoms. As a result, Compton argued, the photons actually perform a random walk, satisfying a diffusion equation, rather than escaping ballistically. The escape time for diffuse propagation is larger than the one for ballistic propagation. Hence the name "radiation trapping".

The good news for atomic gases is that most transitions are radiative, because of the relatively low density of atoms. This implies that no light is lost. However, the matter is quantum mechanical and couples to degrees of freedom over which we have no control. This gives rise to inelastic line broadening, at low temperatures and pressures caused by vacuum fluctuations, and at normal (room) temperatures dominated by atomic collisions and Doppler broadening [16]. The amount of light that is still scattered elastically - the "Rayleigh component" [16] - can be quantified by the albedo defined as the ratio of natural and total line width: $a = \Delta\omega_{\rm nat}/\Delta\omega_{\rm tot} < 1$ [6]. Inelastic line broadening is a specific complication for atomic systems in obeying criterion (2.5). Suppose the light wave travels through the atomic gas, by means of a random walk with diffusion constant D, as envisaged

by Compton. One total scattering event takes one atomic life time τ_0 plus one mean free time to travel to the next atom, which is often much smaller. The diffusion constant is thus estimated to be $D \approx r^2/t \approx \ell^2/\tau_0$. The total time to traverse a distance L - the sample size - is $\Delta t \approx L^2/D \approx (L/\ell)^2\tau_0$. Criterion (2.5) imposes that

$$\left(\frac{L}{\ell}\right)^2 \tau_0 < \tau_\phi \tag{2.10}$$

for the photons to behave mesoscopically. But at the same time we want the medium to be sufficiently inhomogeneous to have multiple scattering, i.e. $L > \ell$. The large factor $(L/\ell)^2$ in criterion (2.10) shows that *dephasing is much more sensitive in multiple scattering than it is in single scattering.* In the last case we would simply impose the natural decay time to be less than the inelastic time or, equivalently, the natural line width to exceed the inelastic line width. Since $\tau_0 \approx \tau_\phi \approx 10^{-8}$ s and $L/\ell > 50$, radiation trapping is far from being mesoscopic. Indeed, Holstein started out with the transport equation (2.6), describing the light waves in the atomic gas as if they were soccer balls in a forest.

The inelastic nature of the light is responsible for one very anomalous feature in multiple light scattering. For purely elastic light scattering it is well know that the step length distribution $P(r)$ of a wave between two successive scattering events is given by an exponential distribution [17]

$$P(r) = \frac{1}{\ell(\omega)} \exp\left(-\frac{r}{\ell(\omega)}\right) , \tag{2.11}$$

featuring the mean free path ℓ at frequency ω. However, an inelastic spectral distribution $F(\omega)$ exists around the resonant frequency. For incoherent light we are allowed to add intensities so that Eq. (2.11) generalizes to

$$P(r) = \int \mathrm{d}\omega \frac{F(\omega)}{\ell(\omega)} \exp\left(-\frac{r}{\ell(\omega)}\right) . \tag{2.12}$$

Since $F(\omega)$ and the total atomic cross-section $\sigma(\omega)$ are both Lorentzian around the resonant frequency, we anticipate $F(\omega) \times \ell(\omega) = F(\omega)/n\sigma(\omega) \approx$ to be constant around the resonant transition. It easily follows [15]

$$P(r) \sim 1/r^{3/2} . \tag{2.13}$$

This law is recognized as a *Lévy distribution.* Its long range makes the radiation trapping problem fundamentally different from light diffusion in fog or paint, and its important role in the interpretation of radiation trapping experiments was first discussed by Holstein [15]. In particular, its first moment - defined as *the* mean free path- diverges. Its second moment - related

to the diffusion constant [17] - diverges as well. Photon transport in atomic gases is thus not Brownian after all.

A contemporary challenge is to obey criterion (2.5) with an atomic gas, and to establish the coherence of the light despite the randomness in the locations of the atoms. Among all line broadening mechanisms, radiative line broadening is the only one that can be 100 % elastic and coherent ($\tau_\phi = \infty$), as is the case for a two level system at not too large radiation intensities [16, 18]. Genuine inelastic mechanisms, such as Doppler broadening and collisional broadening can be suppressed by cooling down, now a state-of-the-art technique. For purely elastic scattering one may expect normal diffusion of waves, but now with giant resonant cross-sections and particles (and perhaps even the light) that must be described quantum-mechanically. Unfortunately, a genuine two-level system is not always at hand (Rubidium has degenerated ground and excited states), and one has to cope with Raman contributions. The first result has recently been obtained by the group in Nice [19], who measured coherent backscattering of light from a cold Rubidium gas, deducing a mean free path of $\ell \approx 2$ mm. Coherent backscattering is one of the pilot effects in mesoscopic wave physics, and has been observed with light (see Fig. 9), ultrasound [20], and indirectly in the conductance of electronic conductors [21, 22].

I hope that this experiment will set a new trend for mesoscopic wave mechanics in atomic gases. It was mentioned in the former section that once in the mesoscopic regime, wave mechanics is a universal formalism, insensitive to small specific details of the system. Once in this regime, scattering theory is the most powerful formalism. In the rest of this lecture I will discuss a semi-classical elastic scattering theory for two-level systems, where mesoscopic effects are most apparent.

3 Light scattering from simple atoms

In this section I will introduce classical wave mechanics, and apply it to light scattering from atoms, without actually doing atomic physics. My aim is to establish the vital link between scattering theory and atomic physics, not to do better than atomic physicists. Many familiar concepts will emerge from this classical approach, such as superradiance, excited energy, dipole-dipole coupling, polarizability. This emphasizes the pertinent role of wave mechanics in problems that are sometimes believed to be truly quentum-mechanical.

3.1 Vector Green's function

The wave equation for classical electromagnetic propagation was shown earlier in Table 1. In this equation, $\varepsilon(\mathbf{r})$ is the dielectric constant that can vary in space. Outside scattering objects it is supposed to take its vacuum value

$\varepsilon = 1$. Denoting by $\mathbf{p}$ the operator $-i\nabla$, it is customary in wave mechanics to consider first the following inhomogeneous equation,

$$\frac{\varepsilon(\mathbf{r})}{c_0^2}\partial_t^2 \mathbf{G}(\mathbf{r},\mathbf{p},t,t') - \mathbf{p}\times\mathbf{p}\times\mathbf{G}(\mathbf{r},\mathbf{p},t,t') = \mathbf{I}\,\delta(t-t')\,. \tag{3.1}$$

This equation defines the vector Green's operator $\mathbf{G}(\mathbf{r},\mathbf{p},t,t')$. Its importance for wave mechanics cannot be underestimated, although especially experimentalists often consider this object as a technical element to be avoided. Bad news for them since *the Green's function is wave mechanics*, and I shall discuss its properties in a nut shell.

The vector nature of the electric field makes $\mathbf{G}$ a second-rank tensor in polarization space. Causality imposes it to vanish for $t' < t$, since no waves can exist before the source emits. This favors a Laplace transform, introducing the complex frequency z. Causality makes $G(\mathbf{r},\mathbf{p},z)$ an analytic operator in the "physical" Riemann sheet $\mathrm{Im}\, z > 0$[1]. Resonant excitations in wave propagation must appear as complex poles in $\mathbf{G}(z)$, when continued analytically into the second sheet $\mathrm{Im}\, z < 0$. This can be made more explicit for light propagation in vacuum ($\varepsilon \equiv 1$). Laplace transforming $t - t'$ to z in the physical sheet, yields

$$\mathbf{G}_0(\mathbf{p},z) = \frac{1}{z^2/c_0^2 - \mathbf{p}^2 + \mathbf{pp}}\,, \tag{3.2}$$

with $\mathbf{pp}$ the second rank tensor with components $p_i p_j$. For $z = \omega + i\epsilon$ we conclude that poles occur for $\omega/c_0 = \pm p - i\epsilon$ and for $\omega = -i\epsilon$, all located in the lower half sheet, but infinitely close to the real axis, showing that these are real excitations, with infinite lifetime.

Formally, $\mathbf{G}_0(\mathbf{r},\mathbf{p},z)$ is still an operator, containing the canonical operators $\mathbf{r}$ and $\mathbf{p}$. The matrix element in momentum representation takes the form $\mathbf{G}_0(\mathbf{p},\mathbf{p}',\omega) = \mathbf{G}_0(\mathbf{p},\omega)\delta(\mathbf{p}-\mathbf{p}')$, with

$$\mathbf{G}_0(\mathbf{p},\omega) = \frac{\hat{\mathbf{p}}\hat{\mathbf{p}}}{(\omega+i\epsilon)^2/c_0^2} + \frac{\mathbf{I}-\hat{\mathbf{p}}\hat{\mathbf{p}}}{(\omega+i\epsilon)^2/c_0^2 - p^2}\,. \tag{3.3}$$

The above poles at $\omega/c_0 = \pm p - i\epsilon$ are oppositely propagating plane wave excitations with speed c_0 and arbitrary transverse polarization vector. The pole at $\omega/c_0 = -i\epsilon$ is a purely longitudinal and *static* excitation.

The matrix element

$$\mathbf{G}(\mathbf{r},\mathbf{r}',\omega) = \langle \mathbf{r}|\mathbf{G}(\omega+i\epsilon)|\mathbf{r}'\rangle \tag{3.4}$$

describes the propagation of a spherical wave at frequency ω from $\mathbf{r}$ to $\mathbf{r}'$ in real space. This interpretation gives many complicated expressions in wave

[1] Strictly speaking this statement is only true in the rotating wave approximation, and a second "physical sheet" with $\mathrm{Im}\, z < 0$ can be identified for counter-rotating waves.

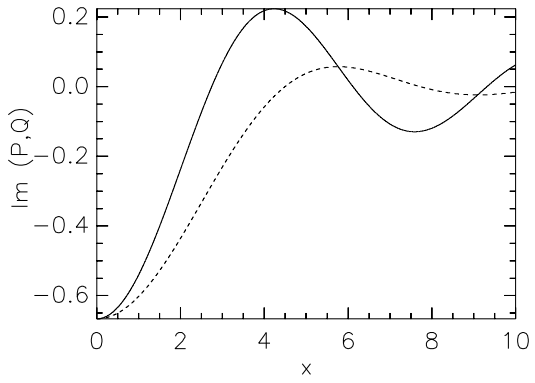

Fig. 2. Imaginary parts of the transverse Green's function P (solid) and the longitudinal Green's function Q (dashed) as a function of distance $x = r\omega/c_0$

mechanics a relatively easy interpretation. In vacuum, $\mathbf{G}_0(\mathbf{r}, \mathbf{r}', \omega)$ depends on the difference $\mathbf{r} - \mathbf{r}'$ only, and can be calculated by Fourier transforming Eq. (3.3). It has a longitudinal part Q, a transverse part P, and a contact term according to,

$$\mathbf{G}_0(\mathbf{r}, \omega) = \frac{\omega}{4\pi c_0}\left[Q\left(\frac{\omega r}{c_0}\right)\hat{\mathbf{r}}\hat{\mathbf{r}} + P\left(\frac{\omega r}{c_0}\right)(\mathbf{1} - \hat{\mathbf{r}}\hat{\mathbf{r}})\right] + \frac{c_0^2\delta(\mathbf{r})}{3\omega^2}\,. \qquad (3.5)$$

with $P(y) = -\exp(iy)[1/y - 1/iy^2 - 1/y^3]$ and $Q(y) = -2\exp(iy)[1/iy^2 + 1/y^3]$. This expression has two important limits. The static regime is defined by $\omega r/c_0 < 1$, whereas the far-field has $\omega r/c_0 > 1$. It can be checked that

$$\mathbf{G}_0(\mathbf{r}, \omega) \rightarrow \begin{cases} c_0^2(4\pi\omega^2 r^3)^{-1}\left[\mathbf{I} - 3\hat{\mathbf{r}}\hat{\mathbf{r}}\right] + c_0^2\delta(\mathbf{r})/3\omega^2 & \text{near field} \\ -(4\pi r)^{-1}[\mathbf{I} - \hat{\mathbf{r}}\hat{\mathbf{r}}]\exp(i\omega r/c_0) & \text{far field} \end{cases}. \qquad (3.6)$$

In the near field, $\mathbf{G}_0(\mathbf{r}, \omega)$ equals the familiar static $1/r^3$ dipole-dipole interaction. The somewhat subtle contact term plays an important role in multiple scattering, as we shall see in section 4. In the far field, the phase $\omega r/c_0$ denotes retardation of the wave. In both regimes, the imaginary part of the Green's function behaves nonsingular, and is - for future purposes - shown in Figure 2.

3.2 An atom as a point scatterer

An atom is very small compared to the resonant wavelength of the light, its "size parameter" $k_0 a_0$ being equal to $1/137$, so we assert the dielectric constant of the atom to be given by the point interaction $\varepsilon(\mathbf{r}) = 1 + \alpha\delta(\mathbf{r} - \mathbf{r}_a)$, where $\mathbf{r}_a$ is the position of the atom. The polarization α has the dimension

of a volume. Point scatterers for classical waves and their applications have been reviewed recently by De Vries *et al.* [23].

We can insert $\mathbf{E}(\mathbf{r},t) = \mathbf{E}(\mathbf{r})\mathrm{e}^{-i\omega t}$ into the Helmholtz equation, and compare the result to the ordinary Schrödinger eigenvalue problem $[p^2 + V(\mathbf{r})]\psi(\mathbf{r}) = E\,\psi(\mathbf{r})$. This comparison identifies ω^2/c_0^2 as the energy E, $[1-\varepsilon(\mathbf{r})]\omega^2/c_0^2 \equiv V(\mathbf{r},\omega)$ as the "electromagnetic potential" and seen to be "energy dependent". Finally, the kinetic operator p^2 is identified with the second rank operator $-\mathbf{p}\times\mathbf{p}\times = \mathbf{p}^2 - \mathbf{pp}$. This comparison is purely mathematical, and just avoids solving the same equation twice. A well-known "solved" result in wave mechanics is the expression for the scattering operator T in terms of the Born series in the potential [24]. Upon carrying out the above modifications for electromagnetic waves, the electromagnetic scattering operator becomes,

$$\mathbf{T}(\omega) = \mathbf{V}(\mathbf{r},\omega) + \mathbf{V}(\mathbf{r},\omega)\cdot\mathbf{G}_0(\mathbf{p},\omega)\cdot\mathbf{V}(\mathbf{r},\omega) + \cdots, \tag{3.7}$$

where $\mathbf{G}_0$ is the vector Green's function in vacuum, introduced in the previous section. The Born series can be interpreted in terms of multiple scattering inside the particle. The series (3.7) are easy to evaluate for the above point interaction. The result is the scattering amplitude is

$$\mathbf{t}_{\mathbf{k}\mathbf{k}'}(\omega) \equiv \langle\mathbf{k}|\mathbf{T}(\omega)|\mathbf{k}'\rangle = -\left[\frac{1}{\alpha}\frac{c_0^2}{\omega^2} + \sum_{\mathbf{p}}\mathbf{G}_0(\mathbf{p},\omega)\right]^{-1}. \tag{3.8}$$

The momentum integral $\sum_{\mathbf{p}} \equiv \int \mathrm{d}\mathbf{p}/(2\pi)^3$ in this expression diverges. The longitudinal catastrophe scales like $c_0^2/\omega^2\,\sum_{\mathbf{p}}\mathbf{pp}/p^2$ and contributes an infinite value to the static polarizability α. We will discard this divergence and say that $\alpha(0)$ is just the measured static polarizability. The transverse catastrophe $\sum_{\mathbf{p}} 1/p^2$ has the dimension of an inverse length scale. Regularizing it by $1/\Gamma$ gives the final form [25],

$$\mathbf{t}_{\mathbf{k}\mathbf{k}'}(\omega) = -\frac{4\pi\Gamma\,\omega^2}{\omega_0^2 - \omega^2 - \frac{2}{3}i\Gamma\omega^3/c_0}, \tag{3.9}$$

where the resonant frequency is defined as $\omega_0^2 \equiv 4\pi\Gamma c_0^2/\alpha(0)$. Expression (3.9) is recognized as the scattering amplitude for a classical radiating dipole [26], provided $\Gamma = r_e$. Thus, the transverse regularization involves the classical electron radius, which is the smallest length scale that can be constructed from classical natural constants, i.e. free from $\hbar$. For this reason, the Bohr radius of the atom disqualifies. In the next section it is established that the lifetime of the excited state equals $(\frac{2}{3}\Gamma\omega_0^2/c_0)^{-1}$. The cross-section for a polarization transition $\mathbf{e}\to\mathbf{e}'$ is proportional to $|\mathbf{e}^*\cdot\mathbf{t}_{\mathbf{k}k'}\cdot\mathbf{e}'|^2 \sim |\mathbf{e}^*\cdot\mathbf{e}'|^2$, and by adding the in-plane ($\mathbf{e}^*\cdot\mathbf{e}' = \cos\theta$) and out-of plane transitions ($\mathbf{e}^*\cdot\mathbf{e}' = 1$) yields the familiar $1+\cos\theta^2$ dipole radiation.

3.3 Polarization, cross-section and stored energy

The best known property that can be calculated from the T-matrix is the extinction cross-section, stating how much light flux is captured by the particle and scattered in some direction, and given by $-\mathrm{Im}\,\mathbf{T}_{\mathbf{kk}}/k$ [6], with $k = \omega/c_0$. Less well known is how material properties are expressed in terms of the T-matrix (3.7) featuring in light scattering theory: the total induced polarization and the totally stored energy of the particle inside a radiation field.

The operator $\varepsilon(\mathbf{r}) - 1$ denotes the polarizability density of the particle and is expressed in terms of the potential as $-\mathbf{V}(\mathbf{r},\omega)c_0^2/\omega^2$. Let $\left|\mathbf{E}_{\mathbf{k}}^+(\omega)\right\rangle$ be the exact "outgoing" eigenfunction of the scattering eigenvalue problem for a normalized incident plane wave $|\mathbf{k}\rangle$ at frequency ω and wave vector $\mathbf{k}$ and some unspecified polarization vector. The induced polarization density is assumed local and linear in the applied electric field, according to the constitutive equation,

$$\left|\mathbf{P}_{\mathbf{k}}^+(\omega)\right\rangle = -\frac{c_0^2}{\omega^2}\mathbf{V}(\mathbf{r},\omega)\,\left|\mathbf{E}_{\mathbf{k}}^+(\omega)\right\rangle\,. \tag{3.10}$$

The total polarizability tensor $\alpha_{\mathbf{k}}(\omega)$ is obtained by integrating the polarization density over the whole particle,

$$\begin{aligned}\alpha(\omega,\mathbf{k}) &\equiv \int \mathrm{d}\mathbf{r}\,\langle\mathbf{r}|\,\mathbf{P}_{\mathbf{k}}^+(\omega)\rangle = -\frac{c_0^2}{\omega^2}\,\langle\mathbf{p}=0|\,\mathbf{T}(\omega)\,|\mathbf{k}\rangle \\ &= -\frac{c_0^2}{\omega^2}\mathbf{T}_{\mathbf{0},\mathbf{k}}(\omega).\end{aligned} \tag{3.11}$$

We have inserted Eq. (3.10) and used the relation $\mathbf{V}\left|\mathbf{E}_{\mathbf{k}}^+\right\rangle = \mathbf{T}\,|\mathbf{k}\rangle$, which is a general result of scattering theory [24]. This equation establishes the link between polarizability α of an arbitrary dielectric particle and its *off-shell* T-matrix. The absorption cross-section, being a property of the far field, involves only the *on-shell* T-matrix, for which $p = k = \omega/c_0$,

$$\sigma(\omega,\mathbf{k}) = -\frac{c_0}{\omega_0}\,\mathrm{Im}\,T_{i\mathbf{k}i\mathbf{k}}(\omega)\,. \tag{3.12}$$

Upon comparing Eqs. (3.11) and (3.12) we conclude that the familiar relation $\sigma \sim \mathrm{Im}\,\alpha$ between polarizability α and absorption cross-section σ breaks down for any finite-size scatterer.

The third property of interest is the stored potential energy V_{stored} inside the scatterer during scattering. Standard methods in atomic physics calculate the vibrational energy of the oscillating dipole [27] or obtain - for a two-level atom - the excited-state density matrix element $\rho_{22}(\omega)$ from the optical Bloch equations [16]. Scattering theory provides rigorous expressions, which have been successfully applied to Mie scatterers (dielectric

spheres) [6]. The method of finding the totally accumulated energy around a dielectric scatterer follows a similar one, originally due to Friedel, applied to the accumulation of charge around an impurity in the solid state [28]. For an incident plane wave with wavenumber $\mathbf{k}$ and polarization i, the totally stored electromagnetic energy around the scatterer is defined as

$$V_{\text{stored}}(\omega) = \int \mathrm{d}\mathbf{r} \left[\varepsilon(\mathbf{r})|\mathbf{E}_{i\mathbf{k}}(\omega)|^2 - 1\right] . \tag{3.13}$$

The "-1" subtracts the normalized incident energy density of the plane wave. In stationary situations, total electric and total magnetic energy can be shown to be equal, as has been supposed in Eq. (3.13)

Scattering theory relates the stored energy to the (far-field) scattering amplitude, and in particular to its phase shift ϕ [29], according to

$$V_{\text{stored}}(\omega) = -\frac{c_0^2}{2\omega^2}\frac{\mathrm{d}}{\mathrm{d}\omega}\omega \mathrm{Re}\, T_{i\mathbf{k}i\mathbf{k}} + c_0 \sum_j \int \mathrm{d}\Omega' \, \frac{\mathrm{d}\sigma}{\mathrm{d}\Omega}(i\mathbf{k} \to j\mathbf{k}') \, \frac{\mathrm{d}\phi}{\mathrm{d}\omega} . \tag{3.14}$$

Herein, $\mathrm{d}\sigma/\mathrm{d}\Omega = |T_{i\mathbf{k}\to j\mathbf{k}'}|^2/(4\pi)^2$ is the differential cross-section for a scattering event from polarization i and wave number $\mathbf{k}$ to j and $\mathbf{k}'$ [24]; ϕ denotes the phase shift of the scattering amplitude for the same transition. The first term in Eq. (3.14) is a somewhat subtle contribution from the forward channel that does not really scatter. The stored energy allows to estimate the typical time scale of the scattering process. Since σc_0 is the energy leaving the particle per unit of time, we can define the (Wigner) *time delay* in the scattering process as,

$$\tau_d(\omega) \equiv \frac{V_{\text{stored}}(\omega)}{\sigma(\omega) c_0} . \tag{3.15}$$

This relation can actually serve to get a heuristic explanation for Eq. (3.14) [6].

For the "atom", whose t-matrix is given by Eq. (3.9), no difference exists between on-shell and off-shell t-matrix. Hence,

$$\alpha(\omega) = -\frac{c_0^2}{\omega^2} t(\omega) , \tag{3.16}$$

and we recover the well-known relation between scattering amplitude and polarization of the harmonic oscillator. Similarly, insertion of Eq. (3.9) into Eq. (3.14) yields,

$$V_{\text{stored}}(\omega) = \frac{c_0^4}{\alpha(0)} \frac{(4\pi\Gamma)^2}{(\omega_0^2 - \omega^2)^2 + (\frac{2}{3}\Gamma\omega^3/c_0)^2} . \tag{3.17}$$

This result coincides with the one obtained for the matrix element $\rho_{22}(\omega)$ using the optical Bloch equations [16] in the case of pure radiation line

broadening. The total atomic cross-section being $\sigma = |t|^2/6\pi$, the delay time becomes,

$$\tau_d = \frac{6\pi c_0^3}{\alpha(0)\omega^4}\,. \tag{3.18}$$

This time is essentially *constant* in the region $\omega_0 \pm \Delta\omega$ around the resonant frequency. The relation to the spontaneous emission time can be established inserting $\alpha(0)/4\pi = 2|\mathbf{d}|^2/\hbar\omega_0$ [30] in terms of the atomic dipole matrix element $\mathbf{d}$. Hence,

$$\frac{1}{\tau_d} = \frac{4}{3}\frac{|\mathbf{d}|^2\omega_0^3}{\hbar c_0^3} = A\,. \tag{3.19}$$

This is the standard expression for the spontaneous emission coefficient A of a two-level atom in vacuum [27]. Spontaneous emission and time delay near resonance thus coincide numerically for pointlike atoms. In the next section I confirm this statement even for two atoms. Physically however, spontaneous emission and resonant time delay are *not at all* equal, since spontaneous emission is an inelastic process and completely incoherent, triggered by vacuum fluctuations, whereas Eq. (3.19) describes the mesoscopic time delay of an *elastically scattered* wave, and is - contrary to A, also defined far away from resonance.

3.4 Two atoms: dipole-dipole coupling

When two resonant scatterers are located in each others near field, their collective scattering cross-section can be different from the sum of the individual cross-sections. This phenomenon is known as *dependent scattering*. In multiple scattering situations it is an important mechanism for the experimental fact that the scattering mean free path is underestimated by the well-known formula $\ell = 1/n\sigma$, where n is the number density of the particles.

Consider Figure 3, showing a plane electromagnetic wave incident on two "atoms". Apart from being scatterers into the far field, both particles act as point sources for their neighbors. As a result, the T-operator of the total system can be written down as,

$$\mathbf{T} = \frac{t\ |1\rangle\langle 1| + t\ |2\rangle\langle 2| + t^2\mathbf{G}_0(\mathbf{r})\ (|1\rangle\langle 2| + |2\rangle\langle 1|)}{1 - t^2\mathbf{G}_0^2(\mathbf{r})}\,. \tag{3.20}$$

In this equation, $\mathbf{r}$ is the interparticle axis, $\mathbf{G}_0(\mathbf{r})$ is a spherical wave propagating from one particle to the other as explained earlier, t is the isotropic scattering amplitude for one particle, as defined in Eq. (3.9), and $|1,2\rangle$ denote the positions of the two pointlike atoms. The denominator $1 - t^2\mathbf{G}_0^2(\mathbf{r})$ signifies all orders of recurrent scattering between the two particles. If $|t^2\mathbf{G}_0^2(\mathbf{r})| > 1$ this factor reduces the scattering amplitude considerably.

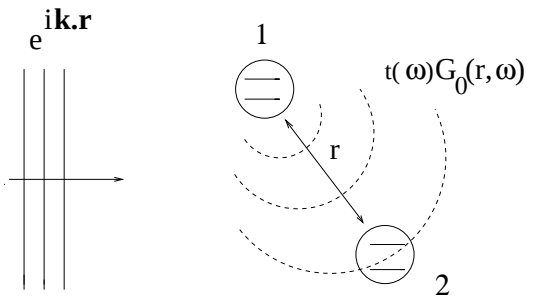

Fig. 3. A plane wave incident on a pair of "two-level" atoms, separated by a distance r. The dashed line denotes a spherical wave scattered by atom 1 towards atom 2 and is given mathematically by $t(\omega)\mathbf{G}_0(\mathbf{r},\omega)$. The scattering amplitude of the two particle system contains all orders in this scattered wave, which induces new scattering resonances.

Since the total scattering cross-section equals $\sigma = |t|^2/6\pi$ and typically $|\mathbf{G}_0| \approx 1/4\pi r$ for not too closely separated atoms, we infer that dependent scattering sets in when $r^2 < \sigma$, i.e. when *the optical volumes overlap*. Near resonance the optical volume is much bigger than the atomic size.

Dependent scattering induces new frequency poles of the scattering amplitude in the complex plane. As customary in atomic physics I define a detuning parameter $\delta = \omega_0 - \omega$. The detuning normalized by the line width $\gamma = \Gamma\omega_0^2/c_0$ I will call Δ. Hence,

$$t(\Delta) = -\frac{4\pi c_0}{\omega_0}\,\frac{1}{\Delta - \frac{2}{3}i}\,. \tag{3.21}$$

For finite $\omega_0 r/c_0$ the pole at $\Delta = \frac{2}{3}i$ splits up into four different poles,

$$\begin{cases} \Delta = \frac{2}{3}i \pm P(\omega_0 r/c_0) \\ \Delta = \frac{2}{3}i \pm Q(\omega_0 r/c_0) \end{cases} \tag{3.22}$$

The quantities P and Q were introduced earlier in Eq. (3.5). Figure 2 shows that $\mathrm{Im}(P,Q) \geq -\frac{2}{3}$, so that all poles ly in the "unphysical Riemann sheet" $\mathrm{Im}\,\omega < 0$, as argued earlier on the basis of causality. The Q-resonances correspond to dressed Σ states with both atomic polarizations along the $\mathbf{r}$-axis. The P solutions have both atomic polarizations perpendicular to the $\mathbf{r}$-axis, and are referred to as the Π-states.

The 4 above poles are reminiscent of the four optical transitions in the famous Dicke problem addressing spontaneous emission from two coupled two-level systems, two of which are "subradiant", and two of which are "superradiant" [31]. The poles that approach the real axis are called *subradiant*. These poles show up as narrow resonances in the joint cross-section,

with large delay time. For $\omega_0 r/c_0 \ll 1$, the subradiant poles correspond to the "+" sign in Eq. (3.22) and tend to genuine bound states. In this regime the Green's function is typically equal to the static dipole-dipole interaction which has $Q \approx -2/y^3$ and $P \approx 1/y^3$, so that subradiant poles occur for $\Delta \approx -2/y^3$, i.e. $\omega = \omega_0[1 + 2\alpha(0)/4\pi r^3]$, and $\Delta \approx 1/y^3$, i.e. $\omega = \omega_0[1 - \alpha(0)/4\pi r^3]$, located at both sides of the resonance ω_0. This outcome is confirmed by the (quantum-mechanical) theory of the resonant Van der Waals interaction between one atom in the ground state and one in the excited state [34].

Poles that move away from the real axis are called *superradiant*. They have a line width twice as large as the one for one atom, reminiscent of the Dicke problem. For large $\omega_0 r/c_0$, all poles finally merge onto the pole at ω_0, with a dominant contribution from the Π-states, for which $\mathrm{Im}\,\omega = -A(1 \pm \frac{3}{2}\sin k_0 r/k_0 r)$. Again, this result also emerges in superradiance from two atoms that are many optical wavelengths apart [32].

In view of the former section, three quantities are of interest: the total cross-section, the total polarization and the stored energy by two atoms, which I shall now obtain. The absorption cross-section is obtained from the forward scattering amplitude using Eqs. (3.20) and (3.12) which I shall average over interparticle direction. This averaging can easily be carried out analytically, and the result is shown in Figure 4 for $\omega_0 r/c_0 = 1$. The two subradiant resonances at both sides of the original resonance ω_0 are clearly visible. Near the atomic resonance ω_0, dependent scattering suppresses the total cross-section of the two particles significantly.

The polarization tensor α of the two particles is readily obtained from Eq. (3.11). Since $\langle \mathbf{p} = 0 | \, 1, 2 \rangle = 1$ it follows that,

$$\alpha_{\mathbf{k}}(\Delta, \mathbf{r}) = \frac{8\pi}{k_0^3} \frac{2\cos\left(\frac{1}{2}\mathbf{k}\cdot\mathbf{r}\right)}{\Delta - \frac{2}{3}i + Q(k_0 r)\hat{\mathbf{r}}\hat{\mathbf{r}} + P(k_0 r)[\mathbf{I} - \hat{\mathbf{r}}\hat{\mathbf{r}}]} \,. \tag{3.23}$$

The polarization tensor is anisotropic, different along and parallel to the interparticle axis. It contains only two poles. For $k_0 r \ll 1$ they are both maximally superradiant. In this classical picture "superradiance" refers to an increased collective radiation damping. The two subradiant transitions hardly suffer from radiation damping since they involve no net excitation of polarization.

The stored energy by the two atoms in an optical radiation field is defined in Eq. (3.13). Also in this case, scattering theory provides a rigorous expression in terms of the forward scattering amplitude $\mathbf{T_{pp}}$ [33]

$$V_{\mathrm{stored}}(\omega) = -\frac{2\pi W_0(\omega) c_0^3}{\omega^3} \mathrm{Im}\,\mathrm{Tr} \sum_{\mathbf{p}} (p^2 - \mathbf{pp}) \cdot \mathbf{G}_0(\mathbf{p}, \omega) \cdot \mathbf{T_{pp}}(\omega) \cdot \mathbf{G}_0(\mathbf{p}, \omega) \,. \tag{3.24}$$

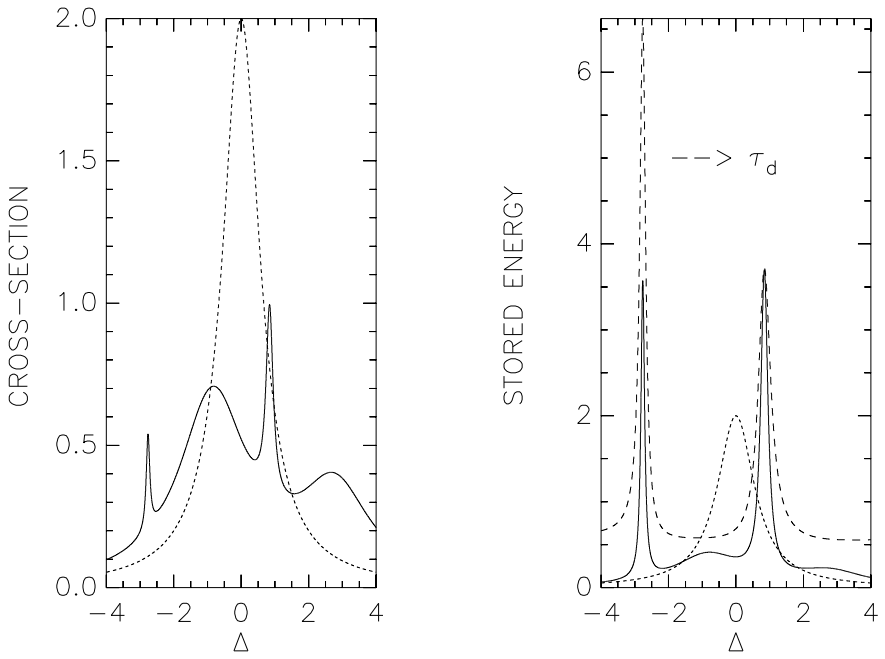

Fig. 4. Total scattering cross-section (left, in units of $6\pi c_0^2/\omega_0^2$, i.e. the resonant cross-section of one atom) and stored energy (right, in units of the resonant value for one atom) for two atoms separated by a distance $r = c_0/\omega_0$. The dotted line in both graphs denotes the Lorentzian profile of two independent atoms far apart. The two subradiant poles are clearly visible. The two superradiant poles give rise to a much broader lob. Near the original resonance ($\Delta \approx 0$) the collective cross-section is suppressed by dependent scattering. The stored energy is very large only near the two subradiant resonances. The line labeled τ_d denotes the delay time defined as $V_{\text{stored}}/\sigma c_0$, in units of the spontaneous emission time for one atom. Away from the subradiant poles it has the constant superradiant value $0.5A^{-1}$

$W_0(\omega)$ denotes the energy density of the background radiation which has been assumed isotropic. Tr denotes a trace over polarization, the tensor $(p^2 - \mathbf{pp})$ guaranteeing that only transverse polarizations come in. Like we saw for the polarization (3.11), evaluation of the above formula requires knowledge of the *off-shell* scattering amplitude. This information is provided by Eq. (3.20) for the atom pair. Straightforward insertion, thereby consistently applying the regularization procedure of the previous section,

yields the relatively simple expression,

$$V_{\rm stored}(\mathbf{r}) = \frac{\pi W_0(\omega) c_0^3}{\omega^2} {\rm Im\,Tr} \frac{\rm d}{{\rm d}\omega} \left[2{\rm Log}\, t(\omega) - {\rm Log}\left(1 - t^2 \mathbf{G}_0^2(\mathbf{r},\omega)\right)\right] . \tag{3.25}$$

The first term just reproduces the stored energy (3.17) of two independent atoms. The second term is the *induced dipole-dipole binding energy* $V_{\rm dd}(\mathbf{r})$. In atomic physics, this binding energy is often described in terms of a "virtual" exchange of a photon between two atoms in the ground state [34]. In Eq. (3.25) this exchange is made explicit by the term $t^2\mathbf{G}_0^2(\mathbf{r})$. It is the first term in a series where high order recurrencies are accounted for by the complex logarithm.

In Figure 4 (right) the stored energy has been evaluated near resonance. Near the subradiant resonances, the delay time τ_d (indicated as a dashed line) becomes very large and would tend to the infinit subradiant value if $\omega_0 r/c_0 \ll 1$. Elsewhere, near the superradiant resonances in particular, the delay time is constant, and equal to the familiar superradiant value of $0.5A^{-1}$.

3.5 Induced dipole force between two simple atoms

By means of the induced dipole-dipole force, an external radiation field can be expected to affect the interaction between two atoms in their ground state. Fedichev *et al.* [35] calculated how the s-wave scattering length is modified by light nearly resonant with a vibrational resonance of two ^{7}Li atoms. I will here estimate the typical interaction strengths involved for a pair of two-level systems with *pure* radiative broadening, and light nearly resonant with the optical transition at ω_0. For an (assumed isotropic) and *purely* monochromatic radiation density W_0, Eq. (3.25) yields, around the resonance ω_0,

$$V_{\rm dd}(\mathbf{r}) = -\frac{W_0 c_0^3}{\Gamma \omega_0^3} {\rm Im\,Tr} \frac{t^3(\Delta)\mathbf{G}_0^2(\mathbf{r},\omega_0)}{1 - t^2(\Delta)\mathbf{G}_0^2(\mathbf{r},\omega_0)} . \tag{3.26}$$

This potential energy is shown in Figure 5. Asymptotically, i.e for $k_0 r > 1$, this potential decays as

$$V_{\rm dd}(\mathbf{r}) \approx \frac{W_0}{k_0^3} \times \frac{1}{\Gamma k_0} \times \frac{1}{\left(\Delta^2 + \frac{4}{9}\right)^{3/2}} \frac{\sin(2k_0 r + \phi)}{(k_0 r)^2} . \tag{3.27}$$

The oscillation factor with wavenumber $2k_0$ is, mostly in the context of impurity screening in the solid state, known as a Friedel oscillation [28]. The factor $1/\Gamma k_0$ denotes the quality factor $\omega_0/\Delta\omega$ of the oscillator. Its large value, $6 \cdot 10^7$ for the optical transition in Rubidium [3], makes the induced dipole energy large. For a typical radiation density $W_0 \approx 10^{-2}$ J/cm^3,

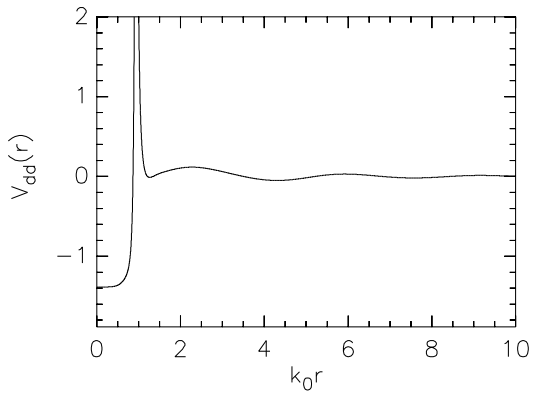

Fig. 5. Induced dipole-dipole energy between two two-level systems tuned one linewidth off-resonance ($\Delta = 1$) in an isotropic radiation field with energy density W_0, as a function of their separation r. Energy unit is $W_0/k_0^3 \times 1/\Gamma k_0$, whose order of magnitude is discussed in the text. The potential is attractive at small distances, reaches a strongly repulsive maximum when a subradiant pole at $k_0 r \approx \Delta^{1/3}$ is excited and asymptotically oscillates as $\sin(2k_0 r)/r^2$.

corresponding to a radiation intensity $I \approx 1$ mW/cm^2 and small enough to avoid saturation effects in Rubidium, we find that $V_{\rm dd} \approx 88K$, 6 orders of magnitude larger than the typical 100 μK associated with the kinetic energy of the atoms! For detunings far off-resonance, and for densities $n \approx 10^{14}$ cm^{-3} we can check that the average distance between the atoms is less than the strong repulsive peak in the dipole-dipole potential, located at $r \approx \Delta^{1/3}/k_0$.

Nearly resonant light has the disadvantage that recoil effects, caused by radiation pressure, are largest [3]. They can be suppressed by lowering the flux density of the incident light. The dipole-dipole energy is proportional to the light flux as well but can, in view of the large quality factor, still largely exceed the kinetic energy of the atoms.

3.6 Van Der Waals Interaction

In this section I discuss the Van der Waals force from the uncustomary point of view of scattering theory, facilitated by the induced dipole-dipole coupling, obtained in Eq. (3.25). In standard textbooks [34], the Van Der Waals Interaction is obtained by perturbing the Hamiltonian of two atoms in their ground state, separated by a distance r, by the standard dipole-dipole interaction varying as $1/r^3$. Second-order perturbation theory leads to a shift of the order of $-1/r^6$ in the energy levels, identified as the attractive Van Der Waals potential.

Equation (3.25) provides the binding energy of two (classical) atoms at distance r, for a incident plane wave with normalized as the dipole-dipole energy. For a general radiation energy density $W(\omega)$ the total dipole-dipole energy is readily seen to be,

$$V_{\rm dd}(\mathbf{r}) = \pi c_0^3 \int_0^\infty {\rm d}\omega \, \frac{\rm d}{{\rm d}\omega} \left(\frac{W(\omega)}{\omega^2} \right) {\rm Im\,Tr\,Log} \left[1 - t^2 \mathbf{G}_0^2(\mathbf{r},\omega) \right] \ , \qquad (3.28)$$

where one partial integration has been carried out. This formula illustrates that a radiation field $W(\omega) \propto \omega^2$ - the case for (classical) thermal radiation at very high temperatures [36] - does not induce a net force. In the absence of any (thermal) background radiation, vacuum fluctuations still contribute an energy density $W(\omega) = \frac{1}{2}\hbar\omega \times \omega^2/\pi^2 c_0^3$, so that

$$V_{\rm dd}(\mathbf{r}) = \frac{\hbar}{2\pi} \int_0^\infty {\rm d}\omega \, {\rm Im\,Tr\,Log} \left[1 - t^2 \mathbf{G}_0^2(\mathbf{r},\omega) \right] \ . \qquad (3.29)$$

A formal series expansion of the complex logarithm shows how subsequent high orders in recurrent scattering contribute to the Van Der Waals potential. Only for the simple two-level system it is possible to sum the whole series of recurrent exchange. The far-field corresponds to $r > 1/k_0$, with $k_0 = \omega_0/c_0$. A straightforward asymptotic analysis shows that low frequencies dominate in Eq. (3.29). Since $t(\omega)\mathbf{G}_0 \sim \omega^3$ this notion also guarantees high orders to be negligible, and

$$\begin{aligned} V_{\rm dd}(\mathbf{r}) &= -\frac{\hbar}{2\pi} \left(\frac{\alpha(0)}{4\pi} \right)^2 {\rm Im} \int_0^\infty {\rm d}\omega \, \frac{\omega^6}{c_0^6} \left[2P(\frac{r\omega}{c_0})^2 + Q(\frac{r\omega}{c_0})^2 \right] \\ &\sim -\frac{\hbar c_0}{\pi r^7} \left(\frac{\alpha(0)}{4\pi} \right)^2 . \end{aligned} \qquad (3.30)$$

This is recognized as the retarded Casimir-Polder interaction [37]. The retardation is contained in the phase of the Green's functions P and Q in the far field.

In the near field $r < 1/k_0$ retarding phase factors in the Green's function and t-matrix can be neglected. One obtains,

$$\begin{aligned} V_{\rm dd}(\mathbf{r}) = \frac{\hbar}{2\pi} \int_0^\infty {\rm d}\omega \, 2 \log \left[1 - \left(\frac{\alpha(0)}{4\pi r^3} \right)^2 \left(\frac{\omega_0^2}{\omega_0^2 - \omega^2 + i\epsilon} \right)^2 \right] \\ + \log \left[1 - \left(\frac{\alpha(0)}{4\pi r^3} \right)^2 \left(\frac{2\omega_0^2}{\omega_0^2 - \omega^2 + i\epsilon} \right)^2 \right] . \end{aligned}$$

This result is valid for $\alpha(0)/4\pi r^3 < 1$, where $\alpha(0) \approx 4\pi a_0^3/3$. Since $k_0 a_0 \approx 1/137$, there is still a considerable regime $a_0 < r < 1/k_0$ where the nonretarded version of the potential applies. The integration can be carried out

using contour integration and

$$V_{\rm dd}(\mathbf{r}) = -\hbar\omega_0 \left(2\sqrt{\frac{1+\sqrt{1+\xi^2}}{2}} + \sqrt{\frac{1+\sqrt{1+4\xi^2}}{2}} - 3 \right] . \qquad (3.31)$$

I abbreviated $\xi \equiv \alpha(0)/4\pi r^3$. For $\xi \ll 1$ this result coincides with the standard Van der Waals potential $V_{\rm dd}(\mathbf{r}) \sim -K(e^2/r)(a_0/r)^5$ [34]. In the regime $a_0 < r < 1/k_0$ the front factor K changes by only a factor of two. When $r < a_0$ the overlap of the atomic orbitals, not described here, leads to a strong repulsion of the atoms, as made explicit in the Lennard-Jones potential.

4 Applications in multiple scattering

Let us consider a random collection of semi-classical two-level atoms. I assume all "atoms" to be identical and neglect any source of inhomogeneous line broadening. The number density of the "atoms" is denoted by n, and their polarizability is $\alpha(\omega)$. For a point particle, the latter relates directly to the scattering amplitude $t(\omega)$, as shown in Eq. (3.16).

4.1 Effective medium

The first aspect of multiple scattering is the dielectric constant ε_e of the effective medium. This parameter relates the average, macroscopic polarization to the applied electric field, according to,

$$\langle \mathbf{P}(\omega) \rangle = (\varepsilon_e - 1) \langle \mathbf{E}(\omega) \rangle . \qquad (4.1)$$

The brackets denote an ensemble averaging over all positions of the atoms. The "textbook" result [38],

$$\varepsilon_e = 1 + \frac{n\alpha(\omega)}{1 - \frac{1}{3}n\alpha(\omega)} . \qquad (4.2)$$

is the celebrated *Lorentz-Lorenz formula*. A number of very critical comments are in order.

Equation (4.2) is often obtained by adding the microscopic polarizations of the individual atoms inside a big sphere, thereby dealing with the surface charges on the boundary of this sphere, generating the "local field factor" $1/(1 - \frac{1}{3}n\alpha)$ [39]. This treatment is correct for $\omega = 0$, i.e. in electrostatics. For $\omega \neq 0$, in particular at optical frequencies, one is obliged to consider retardation. The exact propagation of light at any frequency between two particles is described by the Green's function (3.5). It is possible to derive the Lorentz-Lorenz formula from rigorous microscopic scattering theory.

An elegant though difficult proof can be found in the standard work by Born and Wolf [38], later modified by Felderhof *et al.* [40] and Lagendijk *et al.* [41]. The recent proofs establish that the local field factor in Eq. (4.2) can be seen as a direct consequence of the subtle contact term in Eq. (3.5). They also show that the Lorentz-Lorenz formula applies *provided* that all dependent scattering is ignored. In the former section I showed that these effects become significant when the optical volumes start to overlap. When that happens, the Lorentz-Lorenz relation is a bad approximation. Morice, Castin and Dalibard [42] and Ruostekoski and Javanainen [43] calculated dependent scattering corrections to ε_e for resonant two-level atoms. As we will see, these corrections are sensitive to the statistics of the atoms and may enable to monitor a Bose-Einstein transition or the formation of a Fermi gas.

The second critical remark relevant to relation (4.2) involves the exact role of ε_e in the context of mesoscopic wave physics. This role can only be elucidated with scattering theory. The effective-medium dielectric constant describes the ensemble-averaged field. It is readily checked that ε_e is complex-valued, with *positive* imaginary part. Thus, the average electromagnetic field suffers from *extinction*. Inserting the constitutive relation (4.1) into Maxwell's equations provides a complex dispersion law, relating wave number k and frequency ω of an excitation by a point source $\exp(-i\omega t)\exp(iKr)/r$,

$$K^2 \equiv \left(k + \frac{i}{2\ell}\right)^2 = \varepsilon_e(\omega)\frac{\omega^2}{c_0^2}\,. \tag{4.3}$$

As shown by Loudon [2], the resonant frequency dependence of the real part of the complex wave number K, $k(\omega)$, leads to a familiar polariton behavior, with a pseudo-gap opening up near the resonant frequency. The positive imaginary part of K is translated to an *extinction length* ℓ and is a good example of the discussion on "decoherence", "randomness" and "absorption" in section 2. All three mechanisms contribute to extinction, and by looking at ε_e *alone* no distinction can be made. The parameter ε_e is *not* associated with the (ensemble-averaged) energy density W, and $\mathrm{Im}\,\varepsilon_e$ does not necessarilly imply absorption. The extra knowledge that we started out with, a harmonic oscillator with pure radiative line broadening, leads us to conclude that here, the positive imaginary part must be due to "randomness", making the phase a random variable, and described by the mean free path introduced earlier in Eq. (2.4). On the contrary, in strongly condensed matter, $\mathrm{Im}\,\varepsilon_e$ refers to genuine absorption, expressed by the absorption time τ_a defined in Eq. (2.9). In radiation trapping, the extinction mean free path refers to pure inelastic scattering, as expressed by Eq. (2.12). It is very important to keep this confusing, double role of ε_e in mesoscopic wave mechanics in mind.

4.2 Group and energy velocity

The dispersion relation $\omega(k)$ deduced from Eq. (4.3) defines the group velocity,

$$\begin{aligned} v_g(\omega) &\equiv \frac{\mathrm{d}\omega}{\mathrm{d}k} = \frac{c_0^2}{v_p}\left[1 - \frac{nc_0^2}{2\omega}\frac{\mathrm{d}}{\mathrm{d}\omega}\mathrm{Re}\, t(\omega) + \mathcal{O}(n^2)\right]^{-1} \\ &\approx c_0\left[1 + \frac{4\pi n c_0^4}{\omega_0^4\Gamma}\frac{\Delta^2 - \frac{4}{9}}{\left(\Delta^2 + \frac{4}{9}\right)^2}\right]^{-1} . \end{aligned} \tag{4.4}$$

The last approximation applies close to the resonant frequency ω_0; $v_p = \omega/k$ is the phase velocity.

It is well-known that the group velocity describes the speed of the *maximum* of a wave packet, provided that the pulse distortion is not too big [38]. This is a particularly interesting statement in view of formula (4.4). The factor $4\pi n c_0^4/\omega_0^4\Gamma$ can be rewritten as $(4\pi n/k_0^3) \times (\omega_0/\Delta\omega) \equiv P$. The first factor is basically the number of atoms per optical volume at resonance. A typical atomic density in Bose-Einstein experiments is $n = 10^{14}\mathrm{cm}^{-3}$ so that $4\pi n/k_0^3 \approx 0.7$. The second factor is the quality factor of the resonance. It can be large for atomic resonators. Already when the front factor $P > 0.5$, the group velocity has two singular points where it diverges, taking *negative values* in between (see Figure 6). This criterion is easily satisfied with atomic resonators.

The validity of "group velocity" in this anomalous regime is often questioned. However, the anomalous value of the group velocity is not necessarily violating Einstein causality, which imposes that energy transport cannot be faster than c_0. It has been remarked earlier that the effective-medium dielectric constant ε_e, and hence all quantities constructed from it, have no relation to energy transport. Hence, the group velocity does not describe energy transport and Einstein causality cannot be discussed, and no first principle exists why $0 < v_g < c_0$. Negative group velocities were first discussed by Garret and McCumber [44], later followed by an experiment by Chu *et al.* [45], reporting group velocities $v_g \approx -10^6\mathrm{m/s}$. They occur when the peak of the Gaussian pulse emerges from the sample before the peak of the pulse actually enters. Group velocities have recently achieved new interest in acoustic wave propagation [46].

To show that near resonance no causality problems occur, Brillouin [47] and Loudon [16, 48] introduced the energy velocity v_E. This velocity is defined as the ratio of the average Poynting vector $\langle S\rangle$ and the average electromagnetic energy density $\langle W\rangle$,

$$v_E(\omega) = \frac{\langle S(\omega)\rangle}{\langle W(\omega)\rangle} . \tag{4.5}$$

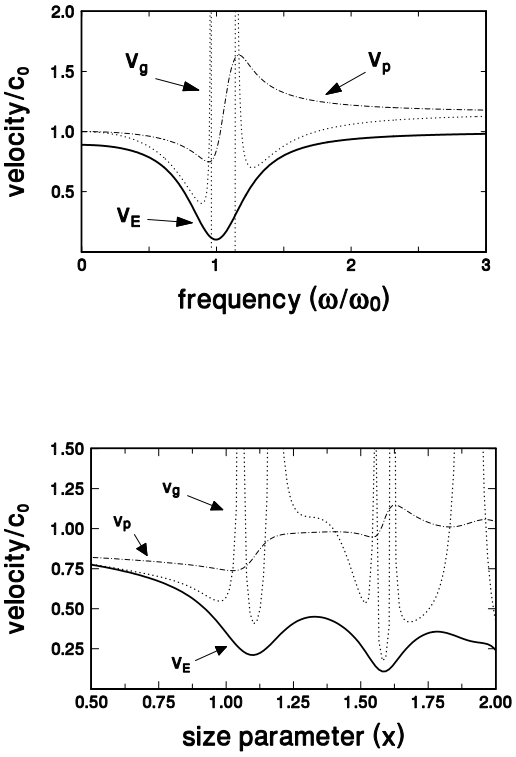

Fig. 6. Phase velocity $v_p = \omega/k$, group velocity $v_g = \mathrm{d}\omega/\mathrm{d}k$ and energy velocity v_E as a function of frequency. Top figure applies to a polariton with resonant frequency ω_0 and atom density $4\pi n/k_0^3 = 1.5$; Bottom figure applies to a random collection of dielectric spheres with index of refraction $m = 2.7$ and volume fraction of 20 %. The parameter $x = a\omega/c_0$ scales the frequency with the size a of the spheres. For simplicity, only the absolute value $|v_g|$ has been plotted. Taken from Lagendijk and Van Tiggelen [6], with thanks to Ad Lagendijk.

The crucial point is that, near a resonance, the energy density achieves a significant and even dominating matter component, signifying the strong delay of light in the scattering process. Inclusion of the matter energy, easily calculated for the harmonic oscillator, confirms that $v_E < c_0$ (Fig. 6).

Since 1990, a derivation of the energy velocity v_E exist using mesoscopic scattering theory [49]. Phenomenological treatments are inadequate if one

wishes to keep track of all the phases. As a bonus, this treatment elucidates what exactly propagates with the energy velocity, something that is not directly clear from the work of Brillouin and Loudon. Nevertheless, scattering theory confirms in great detail the physics behind v_E as it was put forward by Brillouin and Loudon. Quite recently, an asymptotic analysis was published, showing that the peak velocity of the attenuated beam actually approaches the energy velocity when the sample is much larger (typically a hundred times bigger) than the mean free path [52].

The easiest "mesoscopic" derivation of v_E uses arguments of the former sections, and is closest to the original arguments of Brillouin and Loudon. Without the explicit consideration of scattering, the group velocity would equal $v_g = c_0^2 k/\omega = c_0^2/v_p$. Next we must treat the scattering, including the subtle forward scattering, which alone would lead to the group velocity (4.4). The delay time for waves scattererd in arbitrary direction has been given in Eq. (3.15). An elementary argument shows that during multiple scattering, the effective velocity along one mean free path is renormalized by the factor $(\ell/c_0)/[\ell/(c_0^2/v_p) + \tau_d]$. Since $\ell = 1/n\sigma(\omega)$ in terms of the total cross-section $\sigma(\omega)$ of the particles, and using Eq. (3.15) for the delay time, one obtains for the energy velocity,

$$v_E(\omega) = \frac{c_0^2}{v_p} \frac{1}{v_p/c_0 + nV_{\rm stored}(\omega)} \,. \tag{4.6}$$

By using relation (3.14) for $V_{\rm stored}$ in terms of the scattering matrix, one basically recovers the expression for v_E that was originally obtained from transport theory [49], involving the phase-shifts. It applies when dependent scattering can be neglected. Equation (3.14) for the stored energy shows explicitly how the anomalous group velocity term in Eq. (4.4) is compensated by a scattering term, i.e. the group velocity does not count the scattering but that seems to be where most of the energy finally goes near resonant scattering.

Despite the strong similarity of v_E to earlier work, the scattering theory for v_E for classical waves has been subject of a significant and rather technical controversy in literature [50, 51]. It was initiated by a field-theoretical "Ward" identity, valid for electron waves in impurity scattering, stating that the nominator of Eq. (4.6) equals *unity*. It is now known that classical waves do not obey this identity [51], which has to do with their somewhat different conserved quantity. This difference is best be elucidated by splitting the energy $V_{\rm stored}$ stored in one particle up according to

$$V_{\rm stored}(\omega) = \int {\rm d}\mathbf{r} \, \left[|\mathbf{E}(\mathbf{r},\omega)|^2 - 1 \right] + \int {\rm d}\mathbf{r} \, \mathbf{E}(\mathbf{r},\omega) \cdot \mathbf{P}^*(\mathbf{r},\omega) \,, \tag{4.7}$$

where $\mathbf{P}(\mathbf{r},\omega) = [\varepsilon(\mathbf{r},\omega) - 1]\mathbf{E}(\mathbf{r},\omega)$ has been inserted for the local polarization density at frequency ω. The second term signifies stored potential energy inside the scatterer, but does not exist for De Broglie waves.

The first term *cancels* against the term v_p/c_0 in Eq. (3.14) by the "Ward" identity [28], to give 1. The remainder, the potential energy in Eq. (4.7), makes the desired link with the approaches by Loudon and Brillouin, who calculated the vibrational energy of the radiating dipole. Near scattering resonances, $V_{\rm stored}$ becomes large and the velocity v_E small. In Figure 6 I show group and energy velocity for the polariton discussed by Loudon and Brillouin, as well as for an ensemble of Mie scatterers.

The above argument to obtain v_E reveals the role of v_E in the mesoscopic regime. It is the velocity of light measured along *any* long scattering sequence. Long scattering sequences are typically described by a diffusion process, involving a diffusion constant $D(\omega)$. The classical expression for this transport coefficient involves the product of a velocity and a mean free path, the step length of the random walk. The former discussion favors the energy velocity, so that [6,49],

$$D(\omega) = \frac{1}{3} v_E(\omega) \ell^*(\omega) \, . \tag{4.8}$$

This deceivingly simple expression hides the highly mesoscopic nature of v_E and ℓ^*, both subject to interferences. The same equation was derived by Compton back in 1922 [14] for the phenomenon of radiation trapping. In this case, the time delay is just the time is takes for an atom to re-radiate a captured photon inelastically, and also much larger than the mean free time between two captures. The "transport mean free path" ℓ^* differs from the extinction length ℓ if the scattering is anisotropic [53], but for the two-level atom they are just equal. The diffusion coefficient is an experimentally accessible quantity, at least for classical waves, and it is in this way that v_E should be and has been measured directly [49, 54]. The energy velocity also shows up as a typical velocity in *self-induced transparency*, a nonlinear phenomenon due to saturization of the excited level of a two-level system [27], and with a recent report of $v_E \approx 17$ m/s [55].

Values $v_E \approx c_0/10$ have been confirmed by diffusion experiments with visible light [49] and microwaves [54]. The values for v_E measured for classical scatterers are quite smaller than velocities in transparent homogeneous materials, but are still much larger than the ones expected for atomic oscillators. At resonance, the value $v_E/c_0 = 1/[1+9\pi n/k_0^3 \times \omega_0/\Delta\omega]$ is obtained, which can become very small due to the large atomic quality factor. It must be noted that inhomogeneous line broadening decreases the quality factor significantly. In classical wave propagation, a broad size distribution of the particles is often an important source of inhomogeneous line broadening. Cold atoms do not suffer from this. With a atomic density of $n \approx 10^9$ cm^{-3} and an atomic quality factor $\omega_0/\Delta\omega \approx 6 \cdot 10^7$ (Rubidium) a velocity $v_E \approx 3 \cdot 10^{-4}\, c_0$ may be achieved.

4.3 Dipole-dipole coupling in the medium

In section 3.4 I discussed the dipole-dipole energy between two atoms at a fixed distance. The question I address here is how much dipole-dipole binding energy will be stored in a random medium with atom density n. This binding energy provides the leading "dependent scattering" correction to the energy velocity v_E given in Eq. (4.6).

For completely randomly distributed atoms and background radiation with unit energy density, the stored energy density is directly obtained from Eq. (3.25),

$$\langle W_{\rm dd}\rangle = -\frac{1}{2}n^2 \times \frac{\pi c_0^3}{\omega^2}\int {\rm d}\mathbf{r}\,{\rm Im}\,{\rm Tr}\frac{\rm d}{{\rm d}\omega}\,{\rm Log}\left(1-t^2\mathbf{G}_0^2(\mathbf{r},\omega)\right)\,. \qquad (4.9)$$

Similarly, it is possible to obtain the "dependent scattering" correction to the total "absorption" cross-section, using Eqs. (3.20) and (3.12),

$$\langle \delta\sigma_{\rm dd}\rangle = -\frac{c_0}{\omega}\,n\int {\rm d}\mathbf{r}\,{\rm Im}\left(\frac{t^3\mathbf{G}_0^2(\mathbf{r},\omega)+t^4\mathbf{G}_0^3(\mathbf{r},\omega)e^{i\mathbf{k}\cdot\mathbf{r}}}{1-t^2\mathbf{G}_0^2(\mathbf{r},\omega)}\right)_{ii}\,. \qquad (4.10)$$

The first term describes recurrent scatterings back and forth ("loops") to the same atom, averaged over neighbor atoms. The second term has begin and end points on different particles.

Dependent scattering becomes significant when $4\pi n/k_0^3 > 1$[2]. At optical frequencies this requires an atomic density $n > 10^{14}$ cm^{-3}, close to the typical density required for Bose-Einstein condensation. In Figure 7 I show the dependent scattering contributions to stored energy (dashed) and scattering cross-section (solid). A number of features can be remarked. First, both quantities are enhanced on one side ($\Delta < 0$ so $\omega > \omega_0$) and suppressed on the other ($\omega < \omega_0$), leading to a line narrowing. In fact, sumrules imposed by causality impose the frequency integral of both dependent scattering corrections to vanish [56]. This implies that inhomogeneous line broadening will seriously hamper these modifications to the line shape. The structure is caused by the shifts of the subradiant poles in Figure 4 as the distance r is varied.

It was observed by that the Kurchatov group [57,58] that an analytical solution is possible for detunings Δ far off-resonance. In this regime the scattering matrix is $t \approx -4\pi c_0/\omega_0\Delta$. Large detunings have been popular for non-destructive observation of BEC's, since absorption is small. The so-called *quasi-static approximation* assumes that the optical transitions in the atoms are modified by static dipole-dipole interactions with atoms around.

[2] This can be seen by working out the first term of Eq. (4.10), thereby neglecting the denominator, and inserting the far-field expression for the Green's function, given in section 3.1

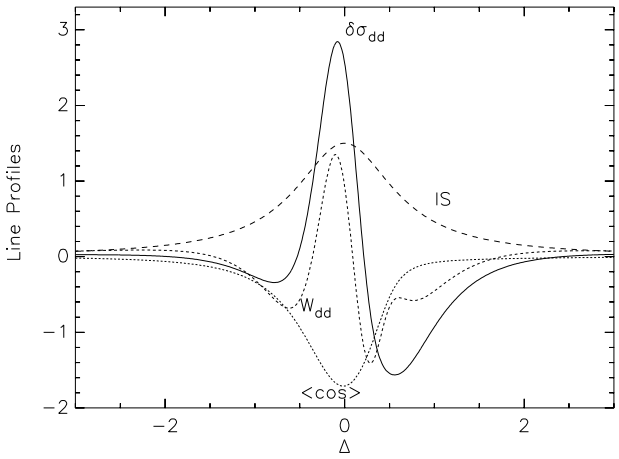

Fig. 7. Dependent scattering corrections (DSC) around the resonant frequency ω_0, due to recurrent scattering from uncorrelated pairs of two-level systems. The corrections have been drawn for an atomic density $4\pi n/k_0^3 = 1$. The curve labeled $\delta\sigma_{dd}$ represents DSC to the absorption cross-section of the atoms (in units of the resonant scattering cross-section $6\pi c_0^2/\omega_0^2$), the curve labeled W_{dd} denotes the dipole-dipole energy density (in units of the quality factor $c_0/\omega_0\Gamma$ of one atom). The curve labeled $\langle\cos\rangle$ measures the anisotropy in scattering from pairs, mainly due to weak localization, as discussed in the text. The curve "IS" represents the Lorentzian homogeneous line shape for a single atom, both for stored energy and cross-section.

In that case the Green's function is approximated by the familiar $1/r^3$ dipolar form, given in Eq. (3.6). The radial integrals in Eq. (4.9) and (4.10) can be done with the result [59]

$$W_{\rm dd}(\Delta) \sim \left(\frac{4\pi n}{k_0^3}\right)^2 \times \frac{1}{\Gamma k_0} \times \frac{1}{\Delta^2}\,, \tag{4.11}$$

$$\Delta\sigma_{\rm dd}(\Delta) \sim \frac{4\pi n}{k_0^3} \times \frac{4\pi}{k_0^2} \times \frac{1}{\Delta^2}\,. \tag{4.12}$$

Since optical absorption and stored energy both scale like $1/\Delta^2$ for independent scatterers as well at large detunings, dipole-dipole interactions start to dominate the wings of the line shape when $4\pi n/k_0^3 > 1$ [60].

4.4 Coherent backscattering

Constructive interferences of waves scattered by two atoms modify the angular distribution of the scattered light. The most important contribution is

drawn in Figure 8a. It describes the constructive interference between two waves scattered from the two particles in opposite order. This phenomenon involves a mesoscopic effect, so-called *coherent backscattering*, that has been extremely well studied with classical waves, most often involving much more particles [20]. For only two atoms, this contribution is easily written down in terms of Green's functions and transition matrices defined in previous sections. A great simplification occurs by supposing that recurrent scattering does not play a role. Then the scattering cross-section for coherent backscattering becomes,

$$\frac{\mathrm{d}\sigma}{\mathrm{d}\Omega}(\mathbf{k}\to\mathbf{k}') = \frac{\mathrm{Tr}}{(4\pi)^2}\, n \int \mathrm{d}\mathbf{r}\ |t|^4\, \mathbf{\Delta}_{\mathbf{k}'}\cdot\mathbf{G}_0(\mathbf{r})\cdot\mathbf{\Delta}_{\mathbf{k}}\cdot\mathbf{G}_0(\mathbf{r})^*\exp[i(\mathbf{k}+\mathbf{k}')\cdot\mathbf{r}]\,. \tag{4.13}$$

The factor $|t|^4$ represents the 4 scattering events, the two Green's functions denote the two waves propagating oppositely from one atom to the other. The two transverse tensors $\mathbf{\Delta}_{\mathbf{k}} = \mathbf{1} - \hat{\mathbf{k}}\hat{\mathbf{k}}$ guarantee polarizations of incident and outgoing electric field to be transverse, the trace summing over all possible polarizations. The last exponential signifies the constructive interference between the scattered waves, and which is perfect at backscattering. An average has been carried out over all neighbor particles 2 that surround particle 1 with number density n. Equation (4.13) contains two complications.

Firstly, the integral in Eq. (4.13) diverges when the atoms are close. This catastrophe is an artifact of having discarded the recurrent scatterings in Eq. (3.20). They introduce a lower cut-off $r \approx \sqrt{\sigma} \leq 1/k$. The phase factor is then of order unity in all directions, and this near-field regime is not expected to be relevant for coherent backscattering. The problem is eliminated by using the far-field expression (3.6) for $\mathbf{G}_0$. For two atoms far apart, the phase factor in Eq. (4.13) is constructive when $(\mathbf{k}+\mathbf{k}')\cdot\mathbf{r} < 1$, i.e. very near backscattering.

Secondly, the integral diverges at large distances exactly at backscattering. Inserting the far-field amplitude, yields

$$\begin{aligned}\frac{\mathrm{d}\sigma}{\mathrm{d}\Omega}(\mathbf{k}\to\mathbf{k}') &\sim \frac{1}{(4\pi)^2}\, n \int \mathrm{d}\mathbf{r}\, \frac{|t|^4}{(4\pi r)^2}\exp(i(\mathbf{k}+\mathbf{k}')\cdot\mathbf{r}) \\ &= \frac{\mathrm{d}\sigma}{\mathrm{d}\Omega}(1)\times\frac{3\pi}{4\ell}\,\frac{1}{|\mathbf{k}+\mathbf{k}'|}\,. \end{aligned}\tag{4.14}$$

The first factor is just the differential cross-section of one atom. Very near back scattering is $|\mathbf{k}+\mathbf{k}'| = 2k\sin\theta/2$ and we obtain a θ^{-1} behavior of the phase function near backscattering. The singularity is integrable and does not lead to a singular total cross-section. Very near backscattering, one should realize that when two atoms are separated by more than than one mean free path ℓ, the coherent backscattering involving only two particles in

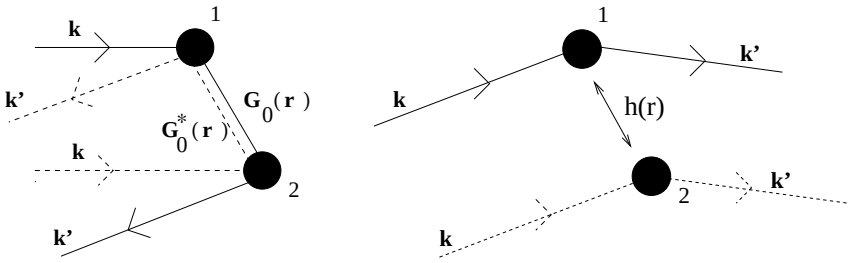

Fig. 8. Two scattering events that modify the angular distribution of the scattered light. Left: Coherent backscattering from two particles. This is a contribution to the scattering cross-section involving at least two particles, and two time-reversed sequences of scattering. The dashed path denotes the path of the complex conjugate wave. The interference between $\psi(1 \to 2)$ and $\psi^*(2 \to 1)$ is constructive at backscattering $\mathbf{k} = -\mathbf{k}'$, and survives any averaging over the positions of particles 1 and 2. Right: Correlation between two particles, with a positive pair correlation function $h(r)$, tends to favor forward scattering.

Figure 8 is seriously hampered. Mathematically this amounts to replacing the Green's function by $\mathbf{G} \sim \exp(ikr)\exp(-r/2\ell)/4\pi r$, with finite extinction. This solves the catastrophe at $\theta = 0$ and reproduces a perfectly well defined line shape with FWHM $\approx 8/k\ell$. For comparison, coherent backscattering from a semi-infinite medium (with all orders of scattering) is known to have the much smaller value FWHM $\approx 0.7/k\ell$ [61, 62]. The reason is that sequences involving n scatterings give much narrower contributions to the cone, because begin and end points are farther apart, typically $\sqrt{n} \times \ell$.

Coherent backscattering from Rubidium has recently been reported for a cold Rubidium gas by Labeyrie *et al.* [19]. The known mean free path is $\ell = 1.8$ mm and the wavelength $\lambda \approx 800$ nm leads to $k\ell = 14.500$. The two-atom prediction is FWHM ≈ 0.5 mrad, very close to the measured value. Since the density is only 10^{10} cm^{-3}, the value $4\pi n/k_0^3 \approx 10^{-4}$ shows that dependent scattering is completely negligible in this experiment. However, coherent backscattering is *not* negligible, because of the extra factor $k\ell$ that is gained by the above regularization of the $1/\theta$ phase function.

The above arguments are quite technical. More rigorous reciprocity arguments show that the coherent enhancement factor must always be of the order of the "background" (i.e. a factor of two enhancement). The basic reciprocity relation for a general T-matrix is [63],

$$T_{\sigma\mathbf{k}\sigma'\mathbf{k}'}(\omega, \mathbf{B}) = T_{\sigma'-\mathbf{k}'\sigma-\mathbf{k}}(\omega, -\mathbf{B})\,, \tag{4.15}$$

In the absence of a magnetic field $\mathbf{B}$, this relation guarantees direct and inverse scattering sequence to interfere constructively for $\mathbf{k} = -\mathbf{k}'$, i.e guarantees an enhancement factor of *exactly* 2, provided that $\sigma = \sigma'$, i.e. when

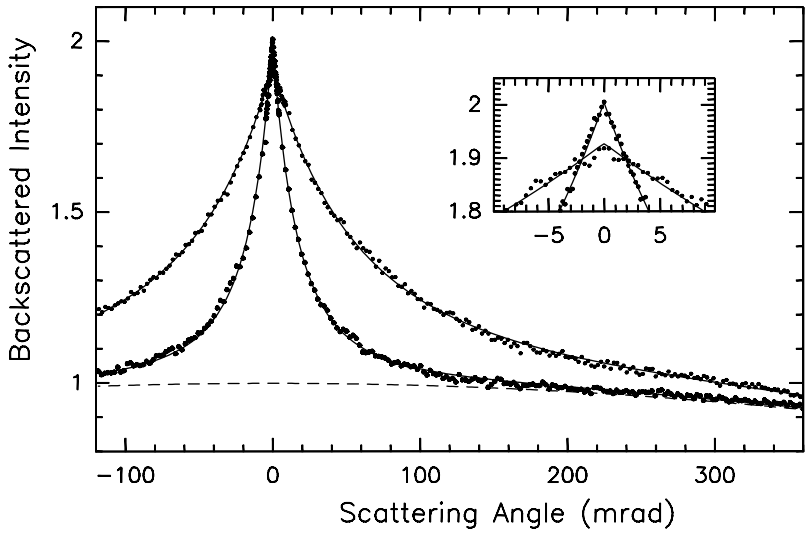

Fig. 9. Coherent backscattering of red light from a disordered slab containing a powder of $BaSO_4$, with a mean free path $\ell = 0.6\,\mu$m (broad curve) and $\ell = 2.1\,\mu$m (narrow curve). Taken from Wiersma, Van Albada, Van Tiggelen and Lagendijk (1995) [69], with thanks to Diederik Wiersma.

input and output deal with the same helicity of the wave.

Several trivial reasons exist why the observed enhancement factor is sometimes less than the one imposed by reciprocity. First, very long orders of scattering lead to a narrow cone, impossible to resolve. Secondly, single scattering does not contribute to the cone, but contributes some 10 % to the background reflection of linearly polarized light. Both effects decrease the enhancement factor. For off-diagonal polarization channels, no symmetry argument exists, and the scrambling of polarization leads to an enhancement factor much smaller than 2 [61, 62, 64]. The possible presence of absorption - or stimulated emission [65] - does *not* affect the reciprocity relation and does therefore in principle not affect the enhancement factor either, although in practice it may come in indirectly via the relative amount of single scattering.

The non-trivial mechanisms that affect coherent backscattering are much more interesting. According to the reciprocity principle (4.15), an external magnetic field destroys coherent backscattering via Faraday rotation of the electromagnetic polarization vector, an effect predicted theoretically by John *et al.* [66] and confirmed experimentally by Maret *et al.* [67]. Dephasing mechanisms and selection rules in Raman transitions are now under study in relation to coherent backscattering in atomic systems [68].

In Figure 9, a cone is presented that was measured with a very accurate angular technique [69]. The used helicity preserving channel has the convenient property that, at least for spherical scatterers, single scattering vanishes. Thus, the experimental enhancement should be exactly two. The inset of Figure 9 confirms the value of two only for $k\ell \gg 1$. The somewhat smaller value for $k\ell \approx 6$ is explained in terms of recurrent scattering. The absence of single scattering in the helicity preserving channel - due to rotational symmetry of the scatterers - does no longer apply to recurrent scattering from two spheres, which break this symmetry. The importance of recurrent scattering is quantified by the value of $4\pi n/k_0^3 \approx 1/k\ell$. The inset of Figure 9 also visualizes the non-analytic line shape at backscattering, as first predicted by Akkermans *et al.* [61, 62] on the basis of the diffusion equation.

The coherent backscattering from two particles demonstrates the collective scattering to become anisotropic. One single two-level system has as much scattering in the forward direction as it has in the backward direction. The angular asymmetry parameter $\langle \cos\theta \rangle$ denotes $\cos\theta$ averaged over the angular phase function, and measures the amount of forward scattering. For individual two-level atoms one has $\langle \cos\theta \rangle = 0$. The curve labeled $\langle \cos \rangle$ in Figure 7 is the result of an exact calculation of the modification by dependent scattering of the angular differential cross-section of two atoms. We notice that $\langle \cos\theta \rangle \approx -4\pi n/k_0^3$ near resonance. The negative value is due to the coherent backscattering effect [56]. It can be expected to suppress diffuse propagation, i.e. lower the diffusion constant.

4.5 Dependent scattering with quantum correlation

Dependent scattering is sensitive to the positions of the two atoms and will change when the positions of the two atoms are correlated, as is for instance the case close to the Bose-Einstein transition. As pointed out in Refs. [42, 57, 58], a measurement of the optical absorption may provide insight into quantum correlations between atoms. Dependent scattering becomes important when $4\pi n/k_0^3 > 1$, making them relevant near Bose-Einstein condensation ($n \approx 10^{14}$ cm^{-3}). The simplest correlations are described by a pair correlation $h(\mathbf{r})$, related to the two-atom distribution function according to $\rho(\mathbf{r}_1, \mathbf{r}_2) = n^2[1 + h(\mathbf{r})]$.

I will illustrate the previous statements for the ideal, homogeneous Bose gas, whose quantum pair function is given by [70],

$$h(\mathbf{r}) = \frac{2n_0}{n} F(\mathbf{r}) + |F(\mathbf{r})|^2 , \tag{4.16}$$

$$F(\mathbf{r}) = \frac{\sum_{\mathbf{k}} n_{\mathbf{k}} \exp(i\mathbf{k}\cdot\mathbf{r})}{n_0 + \sum_{\mathbf{k}} n_{\mathbf{k}}} . \tag{4.17}$$

Here n_0 denotes the number density of atoms in the condensate, and $n_{\mathbf{k}}$ the

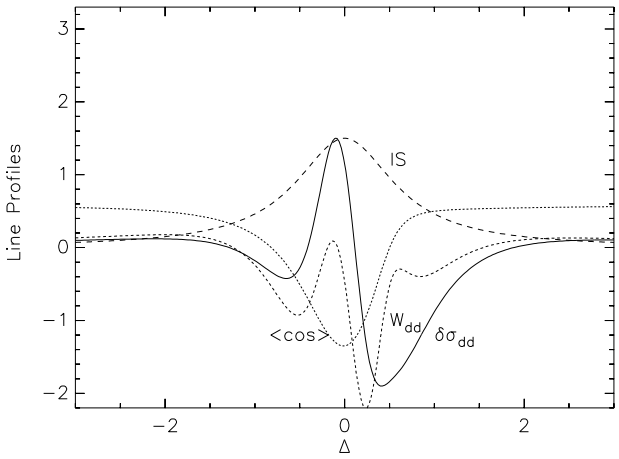

Fig. 10. Dependent scattering corrections (DSC) around the resonant frequency ω_0, due to recurrent scattering from *correlated* pairs of two-level systems (compare to Figure 7, drawn on the same scale). The correction has been calculated for an atomic density $4\pi n/k_0^3 = 1$, and a pair correlation typical at the BEC transition of free bosons. The curve "IS" represents the Lorentzian homogeneous line shape for a single atom, both for stored energy and cross-section.

density in the excited levels. We deduce that $h(0) = 1-(n_0/n)^2$, i.e. beyond the critical temperature it is twice as probable as expected classically to find two atoms on top of each other, but this value decreases below the critical temperature. Far away from the critical temperature, it is easily found that $h(r) = \exp(-\pi r^2/\lambda_B^2)$, with λ_B the De Broglie wavelength. At the critical temperature, it can be checked that $F(r) \approx \lambda_B/r$ so that $h(r) \approx \lambda_B^2/r^2$. For $k_0\lambda_B \approx 1$ and $4\pi n/k_0^3 > 1$, quantum correlations significantly influence line profiles via dependent scattering. Both equalities are obeyed. For Rubidium at $T = 100\,\mu$K we find that $\lambda_B = 0.2\,\mu$m so that $k_0\lambda_B \approx 2.5$, and $4\pi n_c/k_0^3 \approx 2$.

Figure 10 shows stored dipole-dipole energy, dependent scattering cross-section and $\langle\cos\theta\rangle$, displayed earlier in Figure 7, but now for correlated atoms. We have adopted a correlation function $h(r) = 1/(1 + r^2/a^2)$ using $k_0 a = 1$. This correlation function resembles the more complicated one in Eq. (4.17). Upon comparing to Figure 7 the impact of quantum correlations can be estimated. In particular, the line profile of the stored energy is modified. We notice that for $4\pi n/k_0^3 = 1$, these corrections are no longer small, and dependent scattering involving more than only pairs of atoms should be considered.

Bose correlations lead to a *positive* contribution to the angular asymmetry factor $\langle\cos\theta\rangle$, even dominating the negative weak localization correction

for detunings beyond one line width. Indeed, particle correlations induce an angular anisotropy in the collective phase function. This contribution is shown in Figure 8b and reads,

$$\frac{\mathrm{d}\sigma}{\mathrm{d}\Omega}(\mathbf{k}\to\mathbf{k}') = \frac{\mathrm{d}\sigma}{\mathrm{d}\Omega}(1)\times n\int \mathrm{d}\mathbf{r}\, h(r)\exp(i(\mathbf{k}-\mathbf{k}')\cdot\mathbf{r})\,. \qquad (4.18)$$

For a pair correlation $h(r)$ that slowly decays as a^2/r^2 this yields - like was seen in Eq. (4.14) for coherent backscattering - a diverging cross-section θ^{-1}, but now in the *forward* direction. Hence, $\langle\cos\theta\rangle > 0$, independent of Δ. This is confirmed in Fig. 10.

Equations (4.17) and (4.18) can be combined to express pair correlations in terms of the Bose distribution $n_{\mathbf{k}}$ in phase space. If we add the "independent scattering result, we obtain for the collective cross-section,

$$\frac{\mathrm{d}\sigma}{\mathrm{d}\Omega}(\mathbf{k}\to\mathbf{k}') = \frac{\mathrm{d}\sigma}{\mathrm{d}\Omega}(1)\times\sum_{\mathbf{p}_n} n_{\mathbf{p}}\left[1+n_{\mathbf{p}-\mathbf{k}'+\mathbf{k}}\right]\,. \qquad (4.19)$$

The factor $1+n_{\mathbf{p}-\mathbf{k}'+\mathbf{k}}$ signifies pair correlation but can alternatively be regarded as a *stimulated emission* of a boson from a state $\mathbf{p}$ to an already occupied state $\mathbf{p}-\mathbf{k}'+\mathbf{k}$, while the photon is scattered from $\mathbf{k}$ to $\mathbf{k}'$. It was shown by Javanainen [71] that his notion implies that, in the condensated phase, inelastic recoil components show up in the scattered light at both $\omega+\omega_r$ and $\omega-\omega_r$, where $\omega_r = \hbar\Delta\mathbf{k}^2/2m$ is the recoil frequency, and not only at $\omega-\omega_r$.

In the presence of a condensate, the large occupation of the state $\mathbf{p}=0$ yields a cross-section similar to $n_{\mathbf{k}-\mathbf{k}'}\sim 1/\Delta\mathbf{k}^2$. In real space, this corresponds to very long-range $1/r$ behavior in the pair correlation function. Repulsive interactions between the bosons modify this feature somewhat [72], but the consequences for light scattering have so far not been investigated. Recent theoretical research also concentrates on the optics of Fermi-Dirac gazes [73], in which case the stimulated emission factor in Eq. (4.19) achieves a minus sign.

4.6 *From weak towards strong localization*

The modification of transport coefficients by constructive interferences is called *weak localization*, and is one of the most important effects in mesoscopic wave physics. This decrease becomes even more significant when high orders in scattering start to contribute. We shall rely on the following semi-heuristic, but highly mesoscopic argument (Fig. 11). Long paths are described by a diffusion equation. The diffusion Green's function $G_D(\mathbf{r},\mathbf{r}',t)$ satisfies,

$$\left[\partial_t - D\nabla^2\right] G_D(\mathbf{r},\mathbf{r}',t) = \delta(\mathbf{r}-\mathbf{r}')\delta(t)\,, \qquad (4.20)$$

and describes how much wave energy arrives at time t at $\mathbf{r}$ per unit volume after having left $\mathbf{r}$ at time $t = 0$. The return probability $G_D(\mathbf{r}, \mathbf{r}, t)$ can be seen to be inversely proportional to the diffusion constant D. By the reciprocity principle (4.15), the same amount of energy must return due to constructive interference of time reversed waves. This extra term *enhances* the return probability, and should thus lead to a smaller diffusion constant. The typical transverse width of a wave path is of order λ so that during a small interval $\mathrm{d}t$ the relevant volume element to consider is $v_E \mathrm{d}t \times \lambda^2$, with v_E the transport velocity. Upon summing over paths of all lengths, one finds

$$\frac{D_0}{D} \approx 1 + \lambda^2 v_E \int_0^\infty \mathrm{d}t\, G_D(\mathbf{r}, \mathbf{r}, t)\,. \tag{4.21}$$

This result is confirmed by sophisticated transport theories [74], and has been widely used as a starting point for many mesoscopic phenomena [21, 22]. It is a nontrivial outcome as G_D still depends on D by means of Eq. (4.20). For an infinite medium, Eq. (4.20) is easily solved with the result that,

$$\int_0^\infty \mathrm{d}t\, G_D(\mathbf{r}, \mathbf{r}, t) = \int \frac{\mathrm{d}^3\mathbf{q}}{(2\pi)^3} \frac{1}{Dq^2} \approx \frac{1}{(2\pi)^2 D\ell}\,. \tag{4.22}$$

The $\mathbf{q}$-integral diverged for large q, but a cut-off $1/\ell$ has been adopted to avoid low orders of scattering, for which the diffusion equation is not valid. Since $D_0 \sim v_E \ell$ we arrive at,

$$\frac{D}{D_0} \approx 1 - \frac{\text{constant}}{(kl)^2}\,, \tag{4.23}$$

with the constant of order unity. Extrapolating optimistically Eq. (4.23), offers the possibility of a vanishing diffusion constant. This is the weakest among the (many) definitions of *strong localization* [9]. In three dimensions, it is expected to set in when $k\ell \approx 1$, known as the *Ioffe-Regel criterion* of waves. For matter waves at low energy, the cross-section σ reaches the finite value πa^2, with a the s-wave scattering length of the impurity potentials. Thus, localization can be expected at "low energies". For conducting electrons, for which the concept of localization was devised in the first place, the Ioffe-Regel criterion favors the location of the Fermi level near the band edges of the conduction band.

Classical waves have the property that $\sigma \sim \omega^4$ at low frequencies which makes localization very unlikely. For light scattering from nearly resonant atoms, the Ioffe-Regel criterion asserts that $4\pi n/k_0^3 > 1$ to have localization of light, making it an interesting challenge for future experiments with cold gases. A cold Rubidium gas with $n = 10^{14}$ cm^{-3} gives $k\ell \approx 0.28$ at resonance. However, in this strongly scattering regime, dependent scattering

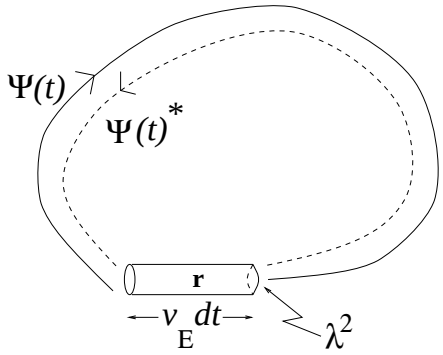

Fig. 11. Schematic representation of constructive interference between two counter-propagating wave paths, long compared to the mean free path. Within a time interval dt, and after a time t they interfere constructively in the small volume element, which enhances the return probability, and lowers the diffusion constant.

must be considered. As evident from Figure 7, dependent scattering may in fact help to *increase* the scattering cross-section somewhat more.

And why not think of the inverse problem of localization of Bose condensed matter waves in a disordered light potential? After all, for such matter waves we should expect $k\ell < 1$ as $k \approx 0$. At present, strong localization has been reported for microwaves and infrared light, as well as for bending waves and acoustic waves (see Ref. [9] for references).

5 Acknowledgments

Most of this work has been carried out with Ad Lagendijk, who I would like to thank for his continuous input. I thank Robin Kaiser, Rodney Loudon, and Ad Lagendijk for the many critical remarks on earlier versions of the manuscript. Discussions with Yvan Castin, Jean Dalibard, Dominique Delande, David Lacoste, Christian Miniatura, Janne Ruostekoski, Rudolf Sprik, Pedro de Vries and Diederik Wiersma are highly appreciated.

References

[1] *New Aspects of Electromagnetic and Acoustic Wave Diffusion*, ed. GDR POAN (Springer-Verlag, Heidelberg, 1998).

[2] R. Loudon, Optics of Ordered and Disordered Atomic Media, in: *Diffuse Waves in Complex Media* ed. J.P. Fouque (Kluwer, Dordrecht, 1999).

[3] R. Kaiser, Cold Atoms and Multiple Scattering, in: *Diffuse Waves in Complex Media* ed. J.P. Fouque (Kluwer, Dordrecht, 1999).

[4] Les Houches session LXI, 1994: *Mesoscopic Quantum Physics*, edited by E. Akkermans, G. Montamboux, J.L. Pichard and J. Zinn-Justin (Elsevier, 1995).

[5] For a recent review: C.W.J. Beenakker, Random Matrix Theory of Quantum Transport, Rev. Mod. Phys. **69**, 731 (1997).

[6] A. Lagendijk and B.A. van Tiggelen, Resonant Multiple Scattering of Light, Phys. Rep. **270**, 143 - 215 (1996).

[7] A.J. Legget, S. Chakravarty, A.T. Dorsey, M.P.A. Fischer, A. Garg and W. Zwerger, Dynamics of the Dissipative Two-State System, Rev. Mod. Phys. **59**, 1 (1987).

[8] for early theoretical and experimental results, see: *Localization, Interaction and Transport Phenomena*, Ed. B. Kramer, G. Bergmann and Y. Bruynserade (Springer, Heidelberg, 1985). Recent results: H. Bouchiat, Experimental Signatures of Phase Coherent Transport, in Ref. [4]

[9] B.A. van Tiggelen, Localization of Waves, in: *Diffuse Waves in Complex Media* ed. J.P. Fouque (Kluwer, Dordrecht, 1999).

[10] S. Chandrasekhar, *Radiative Transfer* (Dover, New York, 1960).

[11] H.C. van de Hulst, *Multiple Light Scattering*, Vols. I and II (Academic, New York, 1980).

[12] D.S. Wiersma, P. Bartolini, A. Lagendijk and R. Righini, Localization of Light in a Disordered medium, Nature **390**, 671 (1997).

[13] A.Z. Genack, P. Sebbah, M. Stoychev, and B.A. van Tiggelen, Statistics of Wave Dynamics in Random Media, Phys. Rev. Lett. **82**, 715 (1999).

[14] K.T. Compton, Phys. Rev. **20**, 283 (1922).

[15] T. Holstein, Imprisonment of Resonance Radiation in Gases, Phys. Rev. **72**, 1212 (1947).

[16] R. Loudon, *The Quantum Theory of Light*, (Oxford, New York, 1991).

[17] A. Heiderich, R. Maynard, A.S. Martinez and B.A. van Tiggelen, Role of Step Length Distribution in Wave Diffusion, Phys. Lett. A **135**, 110 (1994).

[18] C. Cohen-Tannoudji, J. Dupon-Roc, G. Grynberg, *Processus d'Interaction entre Photons et Atomes* (Interéditions, 1988).

[19] G. Labeyrie, C. Müller, C. Miniatura and R. Kaiser, Observation of Coherent Backscattering of Light in Cold Rubidium, to appear in Phys. Rev. Lett. (1999).

[20] G. Maret, Recent Experiments on Multiple Scattering and Localization of Light, in: Ref. [4] (1995). See also Ref. [1] for a recent review on coherent backscattering.

[21] D. Yu. Sharvin and Yu.V. Sharvin, Magnetic-flux Quantization in a Cylindrical Film of a Normal Metal, JETP Lett. **34**, 272 (1981).

[22] B.L. Altschuler abd B.D. Simons, Universalities: from Anderson Localization to Quantum Chaos, in Ref. [4].

[23] P. de Vries, D.V. van Coevorden, and A. Lagendijk, Point Scatterers for Classical Waves, Rev. Mod. Phys. **70**, 447 (1998).

[24] R.G. Newton, *Scattering Theory of Waves and Particles*, (Springer-Verlag, New York, 1982).

[25] Th.M. Nieuwenhuizen, A. Lagendijk and B.A. van Tiggelen, Resonant Point Scatterers in for Multiple Scattering of Classical Wave, Phys. Lett. **A169**, 191 (1992).

[26] J.D. Jackson, *Classical Electrodynamics* (Wiley, New York, 1975).

[27] L. Allen and J.H. Eberly, *Optical Resonance and Two-level Atoms* (Dover, 1987).

[28] G.D. Mahan, *Many Particle Physics* (Plenum, New York, 1980).

[29] B.A. van Tiggelen and E. Kogan, Analogies between Light and Electrons, Friedel's Identity and Density of States, Phys. Rev. A. **49**, 708 (1994).

[30] E. Merzbacher, *Quantum Mechanics* (John Wiley, 1970, 2nd edition), formula 11.86.

[31] R.H. Dicke, Coherence in Spontaneous Radiation Processes, Phys. Rev. **93**, 99 (1954).

[32] Theory: R.G. Brewer, Two-ion Superradiance Theory, Phys. Rev. A **52**, 2965 (1995); Experiment: R.G. DeVoe and R.G. Brewer, Observation of Superradiant and Subradiant Spontaneous Emission of Two Trapped Ions, Phys. Rev. Lett. **76**, 2049 (1996).

[33] Unpublished result as far as I know; Proof is available upon request.

[34] C. Cohen-Tannoudji, B. Diu and F. Laloë, *Méchanique Quantique* (Hermann Éditeurs des Sciences, 1973).

[35] P.O. Fedichev, Yu. Kagan, G.V. Shlyapnikov and J.T.M. Walraven, Influence of Nearly Resonant Light on the Scattering Length in Low-Temperature Atomic Gases, Phys. Rev. Lett. **77**, 2913 (1996).

[36] G.B. Rybicki and A.P. Lightman, *Radiative Processes in Atrophysics* (John Wiley, New York, 1979).

[37] E.A. Power and T. Thirunnamachandran, Casimir-Polder Potential as an Interaction Between Induced Dipoles, Phys. Rev. A **48**, 4761 (1993).

[38] M. Born and E. Wolf, *Principles of Optics* (Pergamon, Exford, 1975).

[39] D.E. Aspnes, Local Field Effects and Effective-medium Theory: a Microscopic Perspective, Am. J. Phys. **50**, 704 (1982).

[40] B.U. Felderhof, G.W. Ford and E.G.D. Cohen, Clausius-Mossotti Formula and its Nonlocal Generalizations for a Dielectric Suspension of Spherical Inclusions, J. Stat. Phys. **33**, 241 (1983).

[41] A. Lagendijk, B. Nienhuis, B.A. van Tiggelen and P. de Vries, Microscopic Derivation of the Lorentz-Cavity in Dielectrics, Phys. Rev. Lett. **79**, 657 (1997).

[42] O. Morice, Y. Castin and J. Dalibard, The Refractive Index of a Dilute Bose Gas, Phys. Rev. A **51**, 3896 (1995).

[43] J. Ruostekoski and J. Javanainen, Lorentz-Lorenz Shift in a Bose-Einstein Condensate, Phys. Rev. A **56**, 2056 (1997).

[44] C.G.B. Garret and D.E. McCumber, Propagation of a Gaussian Light Pulse through an Anomalous Dispersion Medium, Phys. Rev. A **1**, 305 (1970).

[45] S. Chu and S. Wong, Linear Pulse Propagation in an Absorbing Medium, Phys. Rev. Lett. **48**, 738 (1982).

[46] J.H. Page, P. Sheng, H.P. Schriemer, I. Jones, X. Jing and D.A. Weitz, Group Velocity in Strongly Scattering Media, Science **271**, 634 (1996); M.L. Cowan, K. Beaty, J.H. Page, Z. Liu and P. Sheng, Group Velocity of Acoustic Waves in Strongly Scattering Media, Phys. Rev. E **58**, 6626 (1998).

[47] L. Brillouin, *Wave Propagation and Group Velocity* (Academic, New York, 1960).

[48] R. Loudon, The Propagation of Electromagnetic Energy through an Absorbing Dielectric, J. Phys. A **3**, 233 (1970).

[49] M.P. van Albada, B.A. van Tiggelen, A. Lagendijk, and A. Tip, Speed of Propagation of Classical Waves In Strongly Scattering media, Phys. Rev. Lett. **66**, 3132 (1991).

[50] Yu.N. Barabanenkov and V.D. Ozrin, Comment on the Problem of Light Diffusion in Random Media, Phys. Rev. Lett. **69**, 1364 (1992).

[51] B.A. van Tiggelen, A. Lagendijk and A. Tip, Reply to Ref. [50], Phys. Rev. Lett. **69**, 1365 (1992).

[52] K.E. Oughstun and C.M. Balictsis, Gaussian Pulse Propagation in a Dispersive Absorbing Dielectric, Phys. Rev. Lett. **77**, 2210 (1996).

[53] P. Sheng, *Introduction to Wave Scattering, Localization, and Mesoscopic Phenomena* (Academic, San Diego, 1995).

[54] M. Stoychev, N. Garcia, and A.Z. Genack, Electromagnetic Resonances in Low Density Collections of Dielectric Spheres, in: *OSA TOPS on Advances in Optical Imaging and Photon Migration 1996*, ed. R.R. Alfano and J.G. Fujimoto (OSA, Washington, DC, 1996).

[55] L.V. Hau, S.E. Harris, Z. Dutton, C.H. Behroozi, Slow Light in Cool Atoms, Nature **397**, 594 (1999)

[56] B.A. van Tiggelen and A. Lagendijk, Resonantly Induced Dipole-Dipole Interactions in Diffusion of Scalar Waves, Phys. Rev. B **50**, 16732 (1994).

[57] Yu. Kagan, B.V. Svistunov and G.V. Shlyapnikov, Quantum Correlations in the Optical Characteristics of Low-temperature H and D Gases, Sov. Phys. JETP Letters **48**, 56 (1988).

[58] B.V. Svistunov and G.V. Shlyapnikov, Effect of Bose-Einstein Condensation on Resonance Optics in Gaseous H, Sov. Phys. JETP **71**, 71 (1990).

[59] Th.M. Nieuwenhuizen, A.L. Burin, Yu. Kagan, and G.V. Shlyapnikov, Light Propagation in a Solid with Resonant Atoms at Random Positions, Phys. lett. A **184**, 360 (1994).

[60] V.A. Sautenkov, H. van Kampen, E.R. Eliel, and J.P. Woerdman, Dipole-Dipole Broadened Line Shape in a Partially Excited Dense Atomic Gas, Phys. Rev. Lett. **77**, 3327 (1996).

[61] E. Akkermans, P.E. Wolf and R. Maynard, Coherent Backscattering of Light by Disordered Media, Phys. Rev. Lett. **56**, 1471 (1986).

[62] E. Akkermans, P.E. Wolf, R. Maynard and G. Maret, Ref. [61] in detail, J. Phys. (Paris) **49**, 77 (1988)

[63] B.A. van Tiggelen and R. Maynard, Reciprocity and Coherent Backscattering of Light, in : *Wave Propagation in Complex Media* (IMA Volume 96), ed. G. Papanicolaou (Springer, 1997).

[64] M.P. van Albada, M.B. van der Mark and A. Lagendijk, Polarisation Effects in Weak Localisation of Light, J. Phys. D: Appl. Phys. **21**, S28 (1988).

[65] D.S. Wiersma, M.P. van Albada and A. Lagendijk, Coherent Backscattering of Light from Amplifying Media, Phys. Rev. Lett. **75**, 1739 (1995).

[66] F.C. MacKintosh and S. John, Coherent Backscattering in the Presence of Time-reversed and Parity-nonconserving Media, Phys. Rev. B **37**, 1884 (1988).

[67] F.A. Erbacher, R. Lenke and G. Maret, Coherent Backscattering of Light in Magneto-active Media, Europhys. Lett. **21**, 551 (1993).

[68] D. Delande, R. Kaiser, Ch. Miniatura and C. Müller, private comminication.

[69] D.S. Wiersma, M.P. van Albada, B.A. van Tiggelen and A. Lagendijk, Experimental Evidence for Recurrent Scattering in Disordered Media, Phys. Rev. Lett. **74**, 4193 (1995).

[70] Kindly provided by Yvan Castin.

[71] J. Javanainen, Spectrum of Light Scattered from a Degenerate Bose gas, Phys. Rev. Lett. **75**, 1927 (1995).

[72] see: E.M.Lifshitz and L.P. Pitaevskii, *Statistical Physics*, section "superfluidity" (Pergamon, 1991).

[73] J. Ruostekoski and J. Javanainen, Optical Linewidth of a Low Density Fermi-Dirac Gas, preprint (1999).

[74] D. Vollhardt and P. Wölfle, Self-consistent Theory of Anderson Localization, in: *Electronic Phase Transitions*, ed. W. Hanke and Yu. V. Kopaev (North-Holland, Amsterdam, 1992).